AN ABSTRACT OF THE THESIS OF

Ravi Challa for the degree of Master of Science in Civil Engineering presented on December 2, 2010.

Title: Contact and Impact Dynamic Modeling Capabilities of LS-DYNA for Fluid-Structure Interaction Problems

Abstract approved:

Solomon C. Yim

Abstract:

Fluid-structure interaction (FSI) is a very interesting and challenging multi-disciplinary field involving interaction of a movable or deformable structure with an internal or surrounding fluid flow. FSI plays a pivotal role in many different types of real-world situations and practical engineering applications involving large structural deformation and material or geometric nonlinearities. Modeling the ocean environment (deep and shallow water, and surf and beach zones), and loads and motions of platforms and deployed systems accurately or studying the dynamic response of a rigid object as it impacts the water surface are some of the applications of FSI addressed in this research.

Report Documentation Page

Form Approved
OMB No. 0704-0188

1. REPORT DATE	2. REPORT TYPE	3. DATES COVERED
02 DEC 2010		**00-00-2010 to 00-00-2010**

4. TITLE AND SUBTITLE	5a. CONTRACT NUMBER
Contact and Impact Dynamic Modeling Capabilities of LS-DYNA for Fluid-Structure Interaction Problems	5b. GRANT NUMBER
	5c. PROGRAM ELEMENT NUMBER
6. AUTHOR(S)	5d. PROJECT NUMBER
	5e. TASK NUMBER
	5f. WORK UNIT NUMBER
7. PERFORMING ORGANIZATION NAME(S) AND ADDRESS(ES) **Oregon State University,Corvallis,OR,97331**	8. PERFORMING ORGANIZATION REPORT NUMBER
9. SPONSORING/MONITORING AGENCY NAME(S) AND ADDRESS(ES)	10. SPONSOR/MONITOR'S ACRONYM(S)
	11. SPONSOR/MONITOR'S REPORT NUMBER(S)

12. DISTRIBUTION/AVAILABILITY STATEMENT
Approved for public release; distribution unlimited

13. SUPPLEMENTARY NOTES

14. ABSTRACT

Fluid-structure interaction (FSI) is a very interesting and challenging multi-disciplinary field involving interaction of a movable or deformable structure with an internal or surrounding fluid flow. FSI plays a pivotal role in many different types of real-world situations and practical engineering applications involving large structural deformation and material or geometric nonlinearities. Modeling the ocean environment (deep and shallow water, and surf and beach zones), and loads and motions of platforms and deployed systems accurately or studying the dynamic response of a rigid object as it impacts the water surface are some of the applications of FSI addressed in this research. This dissertation is aimed at evaluating the predictive capability of an advanced multi-numerical solution techniques approach to evaluate the contact and impact dynamic modeling capabilities of a finite element code LS-DYNA for Fluid-Structure-Interaction (FSI) problems. To this end, the nonlinear dynamic behavior of water impact of a rigid object is modeled using different numerical methods. The simulations thus far utilize an Arbitrary Lagrangian and Eulerian (ALE) technique and discrete particle model such as the Smoothed Particle Hydrodynamics (SPH) method to capture the multi-physics phenomenon. The dynamics of a water-landing object (WLO) during impact upon water is also presented in this dissertation. Experimental tests for a range of drop heights were performed in a wave basin using a 1/6th scale model of a practical prototype to determine the water impact effects and the results were compared with analytical and numerical predictions. The predictive capability of ALE and SPH features of LS-DYNA for simulation of coupled dynamic FSI responses of the splashdown event of a WLO were evaluated. Numerical predictions are first validated with the original experimental data and then used to supplement experimental drop tests to establish trends over a wide range of conditions including variations in vertical velocity, entry angle and object weight. The reliability of the experimentally measured maximum accelerations was calibrated with classical von Karman and Wagner closed-form solutions and an equivalent-radius approximate analytical procedure is developed and calibrated.

15. SUBJECT TERMS

16. SECURITY CLASSIFICATION OF:			17. LIMITATION OF ABSTRACT	18. NUMBER OF PAGES	19a. NAME OF RESPONSIBLE PERSON
a. REPORT **unclassified**	b. ABSTRACT **unclassified**	c. THIS PAGE **unclassified**	**Same as Report (SAR)**	**116**	

Standard Form 298 (Rev. 8-98)
Prescribed by ANSI Std Z39-18

This dissertation is aimed at evaluating the predictive capability of an advanced multi-numerical solution techniques approach to evaluate the contact and impact dynamic modeling capabilities of a finite element code LS-DYNA for Fluid-Structure-Interaction (FSI) problems. To this end, the nonlinear dynamic behavior of water impact of a rigid object is modeled using different numerical methods. The simulations thus far utilize an Arbitrary Lagrangian and Eulerian (ALE) technique and discrete particle model such as the Smoothed Particle Hydrodynamics (SPH) method to capture the multi-physics phenomenon.

The dynamics of a water-landing object (WLO) during impact upon water is also presented in this dissertation. Experimental tests for a range of drop heights were performed in a wave basin using a $1/6^{th}$ scale model of a practical prototype to determine the water impact effects and the results were compared with analytical and numerical predictions. The predictive capability of ALE and SPH features of LS-DYNA for simulation of coupled dynamic FSI responses of the splashdown event of a WLO were evaluated. Numerical predictions are first validated with the original experimental data and then used to supplement experimental drop tests to establish trends over a wide range of conditions including variations in vertical velocity, entry angle and object weight. The reliability of the experimentally measured maximum accelerations was calibrated with classical von Karman and Wagner closed-form solutions and an equivalent-radius approximate analytical procedure is developed and calibrated.

Contact and Impact Dynamic Modeling Capabilities of LS-DYNA for Fluid-Structure Interaction Problems

by

Ravi Challa

A THESIS

submitted to

Oregon State University

in partial fulfillment of
the requirements for the
degree of

Master of Science

Presented December 2, 2010

Commencement June 2011

Master of Science thesis of Ravi Challa presented on December 2, 2010.

APPROVED:

_____

Major Professor representing Civil Engineering

_____

Head of the School of Civil and Construction Engineering

_____

Dean of the Graduate School

I understand that my thesis will become part of the permanent collection of Oregon State University libraries. My signature below authorizes release of my thesis to any reader upon request.

_____

Ravi Challa, Author

ACKNOWLEDGEMENTS

The author wishes to express his sincere and profound sense of gratitude and respect for his research supervisor Prof. Solomon Yim, Department of Civil and Construction Engineering, Oregon State University for his expert guidance and constant support throughout the period of this research. It is a great opportunity and privilege working under his guidance and the author is especially thankful for his constant encouragement, untiring support and valuable suggestions at every stage of the research work. Foremost, I wish to express my sincere thanks to the Office of Naval Research (ONR) for generously supporting this research work.

I am also thankful to Prof. Harry Yeh and Prof. Merrick Haller for imparting the basic principles in ocean engineering through the challenging course work in water wave mechanics and for agreeing to be a part of my graduate committee. Imposing course work in this area has strengthened my knowledge base and has proven to be an invaluable research tool. Thanks are also due to Prof. Christoph Thomas for agreeing to be a part of my graduate committee. I thank all of them for their critical evaluation and creative suggestions.

The author expresses gratitude to Prof. Odd Faltisen of the Department of Marine Hydrodynamics, Norwegian University of Science and Technology, Trondheim, Norway for his valuable comments during the presentation of both the articles (OMAE-10-20658 and OMAE-10-20659) at the 29th International Conference on Ocean, Offshore and Arctic Engineering, Shanghai, China. His critical comments have helped me successfully

chronicle the equivalent-radius approximate analytical procedure for the rigid object water entry problem.

I am indebted to Prof. Idichandy and Prof. Vendhan, Department of Ocean Engineering, Indian Institute of Technology Madras, India, for introducing me to the astonishing field of ocean engineering in general and computational finite element methods in particular. Their invaluable guidance and perpetual encouragement has been a major contributor in my research carrier. I take this opportunity to specially thank Prof. Idichandy for taking time out despite his busy schedule to travel to Shanghai, China and present the experimental paper on the rigid object water entry (OMAE-10-20658) at the OMAE conference.

I am also thankful to Dr. James Kennedy of KBs2 Inc., California, for providing valuable insights into the contact impact algorithms and in using the ALE and SPH features in LS-DYNA.

This work wouldn‟t have been possible without the excellent support provided by Paul Montagne, Wade Holmes and Mike Sanders from the computing system administration and the high-performance computational platforms of the College of Engineering.

The author would also like to thank the administrative staff of School of Civil and Construction Engineering for being very friendly and helpful with all the department paper work and for their constant encouragement which takes off a lot of stress outside the research periphery.

Thanks are also due to my friends who are the fulcrum of my existence: Divya Valluri, Vineeth Dharmapalan, Sasidhar Nirudodhi, Aruna Narayan, Matthew Hallowell, Gaurav Jat, Ramakrishna Sarangapani, Seshu Nimmala and Suraj Darra (to mention a few) for their love and support.

I am also thankful to all my near and dear ones, relatives and friends who helped me in no small measure to accomplish this target. Importantly, the author wishes to express his sincere gratitude to his Father- Sri Ramamurthy Challa, Mother- Vasundhara Challa, Sister- Lalitha Mallik and Brother-in-law- Mallik Pullela for their unconditional love and affection, not to mention their patient wait to see me accomplish my research.

Finally, I am indebted to ***Shri Shirdi Sai Baba*** *and* ***Maa Durga Shakthi*** for their eternal support in guiding me through the good and testing times and without their blessings, I wouldn‟t have seen this day.

TABLE OF CONTENTS

Page

TABLE OF CONTENTS (Continued)

Page

LIST OF FIGURES

LIST OF FIGURES

LIST OF TABLES

	Guru Gobind Dou Khade	
	Kaake Lagoon Paay	
	Balihari guru aapne	
	Gobind Diyo Batay	

Translation: Guru and God are ever-present and whom shall I bow first?
I shall bow to my mighty Guru as he has shown me the path to God.

---Sant Kabir

Dedication

To Shri Shiridi Sai Baba and Maa Durga Shakthi
and
To my Father, Mother, Sister and Brother-in-Law

Contact and Impact Dynamic Modeling Capabilities of LS-DYNA
For Fluid-Structure-Interaction Problems

Chapter-1: Introduction

1 Introduction

Fluid-Structure Interaction (FSI) is a very interesting and challenging multi-disciplinary field involving interaction of a movable or deformable structure with an internal or surrounding fluid flow. FSI plays a pivotal role in many different types of real-world situations and practical engineering applications involving large structural deformation and material or geometric nonlinearities.

Determining the hydrodynamic forces on a structure or the motion of objects resting on the ocean bottom forms an intrinsic component of any typical FSI problem. Analysis of such problems is extremely difficult and therefore experimental investigations (or empirical laws) by conducting experiments in a physical wave basin. These experiments though impendent with the real world scenario often are time-consuming and expensive. Importantly, it is not economically viable to conduct parametric studies using experiments. Alternatively, numerical models when developed with similar capabilities will complement the experiments very well because of the lower costs and the ability to study phenomena that are not completely feasible in a physical laboratory.

A significant component of the applications of FSI addressed in this work involves the modeling of the dynamic response of a rigid object as it impacts the water surface. This

dissertation is aimed at evaluating the predictive capability of an advanced multi-numerical solution techniques approach to critically evaluate the contact and impact dynamic modeling capabilities of a finite element code LS-DYNA for Fluid-Structure-Interaction (FSI) problems. The dynamics of such water-landing object (WLO) during impact upon water is also presented in this dissertation. The study of hydrodynamic impact between a body/object in motion and water surface finds application in aerospace and ocean engineering fields. The effect of this impact is often prominent in the design phase of the project and, therefore, the importance of studying the event with more accuracy than in the past is imperative. Usually the study of the phenomenon is dealt with experiments, empirical laws, and lately, with finite element simulations. Experimental tests for a range of drop heights were performed in a wave basin using a $1/6^{th}$ scale model of a practical prototype to determine the water impact effects and the results were compared with analytical and numerical predictions.

The numerical simulations thus far utilize an Arbitrary Lagrangian and Eulerian (ALE) technique and discrete particle model such as the Smoothed Particle Hydrodynamics (SPH) method to predict the splashdown event of a WLO. Numerical predictions are first validated with the original experimental data and then used to supplement experimental drop tests to establish trends over a wide range of conditions including variations in vertical velocity, entry angle and object weight. The reliability of the experimentally measured maximum accelerations was calibrated with classical von Karman and Wagner closed-form solutions and an equivalent-radius approximate analytical procedure is developed and calibrated.

2 Literature review

This section reviews the literature to critically evaluate the contact and impact dynamic modeling capabilities of LS-DYNA in simulating the dynamics of a generic rigid-body impacting the water surface. A detailed review of the literature is presented in the following chapters and the list of references is provided in the bibliography section at the end of the dissertation.

2.1 On contact-impact dynamics of a Water Landing Object (WLO)

Studies on impact phenomena based on the theoretical and experimental work by von Karman (1929) resulted in equations for the impact of rigid bodies on a fluid assuming that the reaction of water was solely due to its inertia. The accelerations and pressures affecting the rigid body were estimated using an approximate expression for the added mass due to the presence of the water.

Baker and Westine (1967) conducted experimental investigations on a $1/4^{th}$ scaled model of the Apollo Command Module (ACM) to study the structural response to water impact in both the elastic and failure-initiation regimes. Data from the model tests were compared with results of full-scale experiments.

Kaplan (1968) examined the specific problem of the ACM impacting water. Their theory and experiments showed that the peak acceleration was proportional to the square of the impact velocity and the results correlated well with the full-scale ACM impact tests.

Miloh (1991) obtained analytical expressions for the small-time slamming coefficient and wetting factor of a rigid spherical shape in a vertical water entry using experimental data from the ACM tests. A semi-Wagner approach was proposed and then used to compute

the wetting factor and the Lagrange equations were employed in order to determine the slamming force from the kinetic energy of the fluid. Good agreement between theoretical model and experimental measurements, both for the early-stage impact force and the free-surface rise at the vicinity of the sphere, was observed.

Faltinsen (1997) studied the theoretical methods for water entry of two-dimensional and axisymmetric bodies. A numerical method was developed and compared against asymptotic methods and validated by experiments for cone and sphere shaped objects. The significance of the effect of local rise up of the water during entry was identified.

Brooks and Anderson (1994) investigated the dynamic response of water-landing space module (WLSM) during impact upon water. A $1/5^{th}$-scale model was tested in a three-dimensional (3-D) basin at the Oregon State University Wave Research Laboratory and the results were compared with those obtained using analytical techniques and computer simulations. The 3-D FE model was validated by comparison with previous full-scale test data and theory.

Scolan and Korobkin (2001) considered the 3-D problem of a blunt-body impact onto the free surface of an ideal incompressible liquid based on Wagner‟s theory.

Seddon and Moatamedi (2006) reviewed the work undertaken in the field of water entry between 1929 and 2003, providing a summary of the major theoretical, experimental and numerical accomplishments in the field.

Melis and Khanh Bui (2003) studied the ALE capability to predict splashdown loads on a proposed replacement/upgrade of the hydrazine tanks housed within the aft skirt of a Space Shuttle solid rocket booster. Preliminary studies on the booster impacting water

showed that useful predictions can be made by applying the ALE methodology to a detailed analysis of a 26-degree section of the skirt with proposed tank attached.

Wang and Lyle (2007) simulated the space capsule water landing using an ALE-FE solver and a penalty coupling method to predict the fluid and structure interaction forces. The capsule was assumed rigid and the results were found to correlate well with close form solutions.

Literature for a rigid object water impact acknowledges the fact that the physical interpretation of the problem developed by von Karman formed the basis of nearly all subsequent works hence the existing experimental data is confined to a convex shaped objects impacting water. A lot of literature is available on the water entry of spheres impacting with high velocities and the ensuing cavity formations. However, there is scanty literature available on the water impact of rigid bodies of arbitrary shape especially with low velocities of impact. Literature available on the analysis of the impact scenario using finite element codes such as the LS-DYNA thus far utilizes ALE technique for most of the impact problems but the use of discrete particle method such as SPH was not adopted hitherto for the ditching problems. Though the FE codes were used for many FSI problems in the past, modeling accurate water behavior still poses difficulties.

3 Objective and scope of the present study

For the critical evaluation of the contact and impact dynamic modeling capabilities of LS-DYNA to study the dynamics of a WLO impacting the water surface, the objectives of the present work are manifold:

- Understanding the predictive capabilities of different numerical methods in LS-DYNA (such as ALE and SPH) and to simulate the contact-impact FSI problem
- Developing an advanced multi-physics model with a multi-numerical solution technique approach to predict the nonlinear dynamic behavior of a rigid object impacting the water surface
- Developing a semi-approximate equivalent-radius analytical procedure based on the von-Karman and Wagner closed form solutions and calibrate with experimental results
- Using the ALE and SPH features of a state of the art nonlinear dynamic explicit time integration finite element code (LS-DYNA) to simulate the impact phenomenon and compare it with experimental results
- Conducting performance studies of ALE and SPH in modeling the impact scenario

4 Organization of the thesis

Chapter-2 deals with the experimental investigations and analytical estimates involving drop tests with the scaled model of a WLO. The peak accelerations and peak pressures coming on the WLO were presented and an approximate equivalent radius approach is presented.

Chapter-3 focuses on a numerical study on the dynamic response of a generic rigid WLO during water impact. The predictive capability of the explicit finite-element ALE and SPH methods were evaluated. The numerical predictions are first validated with experimental data for maximum impact accelerations and then used to supplement experimental drop tests.

General conclusions along with a prelude to the continuation of this work are presented in Chapter-4. Major observations pertaining to the modeling aspects of WLO and the extent to which ALE and SPH can simulate the complex event of a rigid object water entry are presented. The computational framework needed to enhance the modeling and prediction of FSI problems are discussed as a part of the future work.

Chapter 2

Rigid-Object Water-Surface Impact Dynamics: Experiment and Semi-Analytical Approximation

Rigid-Object Water-Surface Impact Dynamics: Experiment and Semi-Analytical Approximation

Ravi Challa[1], Solomon C. Yim[2], V.G. Idichandy[3] and C.P. Vendhan[3]

[1]Graduate Student, School of Civil and Construction Engineering, Oregon State University, Corvallis, OR- 97330
[2]Professor, Coastal and Ocean Engineering Program, School of Civil and Construction Engineering, Oregon State University, Corvallis, OR-97330
[3]Professor, Department of Ocean Engineering, Indian Institute of Technology Madras, Chennai-600036

The contents of this paper are based on two articles (OMAE-10-20658 and OMAE-10-20659) presented at the 29th International OOAE Conference in Shanghai, China. Significant revisions and improvements have been made incorporating comments and suggestions from reviewers and discussions with expert researchers at and after the conference presentations.

Abstract

An experimental study of the dynamics of a generic rigid water-landing object (WLO) during water impact and an equivalent-radius approximate analytical procedure is developed and calibrated in this study. The experimental tests in a wave basin covered a range of drop heights using a 1/6th-scale model of a practical prototype for two drop-mechanisms to determine the water impact and contact effects. The first mechanism involved a rope and pulley arrangement while the second mechanism employed an electromagnetic release to drop the object. Hydrodynamic parameters including peak acceleration, touchdown pressure and maximum impact/contact force were measured for various entry speeds (correspondingly various drop heights) and weights of the object. Results from the tests show that the impact acceleration and touchdown pressure

increases approximately linearly with increasing drop height and the data provides conditions that keep impact accelerations under specified limits for the WLO prototype. The experimentally measured maximum accelerations were compared with classical von Karman and Wagner approximate closed-form solutions. In this study, an improved approximate solution procedure using an equivalent radius concept integrating experimental results with the von Karman and Wagner closed-form solutions is proposed and developed in details. The resulting semi-analytical estimates are calibrated against experiment result and found to provide close matching.

1 Introduction

The study of hydrodynamic impact of a moving body on a water free-surface finds variety of applications in the aerospace and ocean engineering fields. The present study is concerned with rigid-object/water-surface impact dynamics of a water-landing object (WLO) in an open ocean using a series of drop tests in a wave basin to assess the maximum force and resulting accelerations. The effect of this impact is prominent in the design phase of the WLO project in determining the maximum design force for material strength determination to ensure structural and equipment integrity and human safety.

Prototype data has been provided by the Indian Space Research Organization (ISRO) to facilitate the making of a physical model of WLO. The prototype used for the Indian space mission is unique in a way that it is conical with a rounded nose (which impacts the water surface first) than compared to the convex shape of the base used for Apollo

Command Module (ACM) for the American space missions. This difference precludes meaningful comparison with existing literature available for ACM.

Studies on impact phenomena based on the theoretical and experimental work by von Karman (1929) resulted in equations for the impact of rigid bodies on a fluid assuming that the reaction of water was solely due to its inertia. The accelerations and pressures affecting the rigid body were estimated using an approximate expression for the added mass due to the presence of the water. Baker and Westine (1967) conducted experimental investigations on a $1/4^{th}$ scaled model of the Apollo Command Module (ACM) to study the structural response to water impact in both the elastic and failure-initiation regimes. Data from the model tests were compared with results of full-scale experiments. Kaplan (1968) examined the specific problem of the ACM impacting water. Their theory and experiments showed that the peak acceleration was proportional to the square of the impact velocity and the results correlated well with the full-scale ACM impact tests.

Miloh (1991) obtained analytical expressions for the small-time slamming coefficient and wetting factor of a rigid spherical shape in a vertical water entry using experimental data from the ACM tests. A semi-Wagner approach was proposed and then used to compute the wetting factor and the Lagrange equations were employed in order to determine the slamming force from the kinetic energy of the fluid. Good agreement between theoretical model and experimental measurements, both for the early-stage impact force and the free-surface rise at the vicinity of the sphere, was observed.

Faltinsen (1997) studied the theoretical methods for water entry of two-dimensional and axisymmetric bodies. A numerical method was developed and compared against asymptotic methods and validated by experiments for cone and sphere shaped objects. The significance of the effect of local rise up of the water during entry was identified.

Brooks and Anderson (1994) investigated the dynamic response of water-landing space module (WLSM) during impact upon water. A $1/5^{th}$-scale model was tested in a three-dimensional (3-D) basin at the Oregon State University Wave Research Laboratory and the results were compared with those obtained using analytical techniques and computer simulations. The 3-D FE model was validated by comparison with previous full-scale test data and theory.

Scolan and Korobkin (2001) considered the 3-D problem of a blunt-body impact onto the free surface of an ideal incompressible liquid based on Wagner"s theory. Seddon and Moatamedi (2006) reviewed the work undertaken in the field of water entry between 1929 and 2003, providing a summary of the major theoretical, experimental and numerical accomplishments in the field.

It is apparent that the physical interpretation of the problem developed by von Karman formed the basis of nearly all subsequent works. The existing experimental data is confined to a convex shaped objects impacting water. In this study, an understanding the dynamics of a conical shaped WLO during water impact was achieved by performing experiments using a $1/6^{th}$ scale model made of fiber reinforced polymer (FRP) simulating water impact through a series of drop tests with varying heights measuring

their maximum impact acceleration, touchdown pressure and impact force. The reliability of the experimentally measured maximum accelerations was calibrated with bounds provided by classical von Karman and Wagner approximate closed-form solutions. In this paper, an improved approximate solution procedure is developed using an equivalent radius concept integrating experimental results, turning the von Karman and Wagner "bounds" into more useful closed-form semi-analytical estimates. The resulting estimates are then calibrated against experimental data.

2 Experimental Investigations of WLO Impact Dynamics Using Drop Tests

The experimental investigations carried out as a part of the present study on the WLO consists of drop tests from a range of heights. To simulate the dynamic behavior of the WLO for the impact experiment, a $1/6^{th}$ Froude scale-model was fabricated, which is essentially a conical shell with rounded nose. The overall configuration of the WLO prototype is shown in Figure 1. Specifications of the prototype and model are shown in Table 1. Note that the conical portion (nose part of the rigid-object) impacts the water surface. The origin is located at the deck of the WLO and the position of Z_{cg} is measured from the flat base (Figure 1).

2.1 Experimental Test Cases

Two independent sets of drop test are conducted in the experiment. Drop test I involved dropping the object using a rope and pulley arrangement, while Drop Test II employed an electromagnetic release to drop the model. Both sets of experiments provide valuable

and complementary experimental data (for different weight distribution ratios) for numerical model calibration.

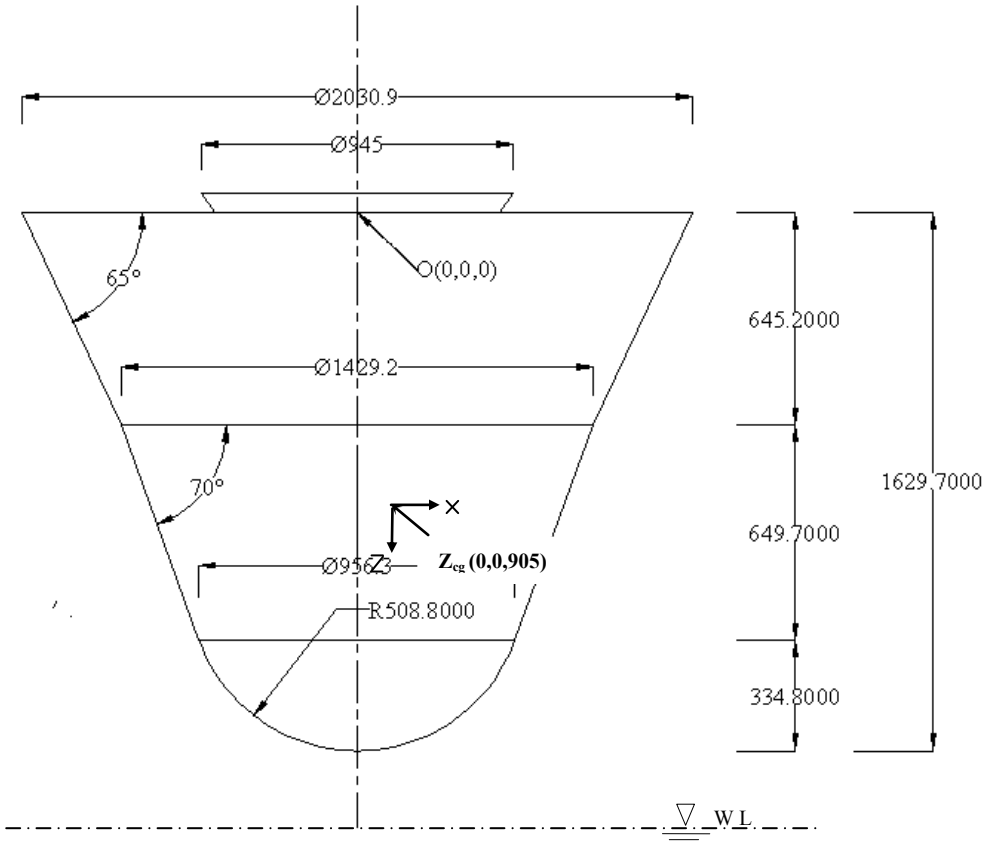

Fig. 1 Overall configuration of WLO Prototype
(All dimensions are in mm)

2.1.1 Drop Test I

The first set of drop tests was performed recently in the wave basin (30m x 30m in plan and 3m deep) at the Department of Ocean Engineering at IIT-Madras under calm water conditions. Given the maximum clearance of the laboratory, the achievable maximum velocity of impact was estimated to be about 9.81m/s. This impact velocity was achieved by dropping the model from an overhead crane with a drop height of 5m above the water

surface. The drop tests were carried out over a range at 0.5m intervals. An important design parameter is the mass, which is selected as 2.03 kg for the test model made of FRP. A skin thickness of 5mm was selected, with extra thickness at the nose (of about 10mm) to withstand the force of impact. The estimated values of the centre of gravity and moment of inertia are given in Table 1. **Appendix-C** shows the inertial properties of the WLO model.

Table 1: Specification of Prototype and Model

Property	Prototype Specifications	Model Specifications
Mass of the object at reentry	450 kg	3.0 kg
Mass without flotation bags and parachute	432 kg	2.03 kg
Thickness of skin	25mm	5mm (extra thickness at nose)
Maximum height of the space capsule	1629.7mm	271.66mm
Maximum diameter of the space capsule	2030.9mm	338.5mm
X_{cg}	0	0
Y_{cg}	0	0
Z_{cg}	890.15mm	147.28mm
I_{xx}	169.38 kg m^2	0.02172 kg m^2
Iyy	170.76 kg m^2	0.02189 kg m^2
Izz	109.44 kg m^2	0.01402 kg m^2

The vertical acceleration of the model was measured on impact by using an accelerometer, placed at the center of gravity (CG) of the model. A 5-bar strain gauge-

type pressure transducer (mounted at the nose tip with a measuring area of 15 mmϕ) is used to calculate the touchdown pressure during impact. The accelerometer and the pressure transducer were connected to amplifiers and a PC based data acquisition system was employed to acquire the data. Both the sensors were accurately calibrated and found to be practically perfectly linear with curve-fitted conversion values of less than 0.5% error [For the accelerometer calibration, 1 Volt corresponds to 11.1g and for the pressure sensor, 1 Volt corresponds to 0.166 bar ($0.166x10^5 Pa$)].

Impact Test Results---The WLO was dropped, nose down, from various heights to determine the acceleration of the model during the impact and to measure the impact pressure at the nose. Ten seconds of data, with a sampling rate ranging from 1,000 Hz to 5,000 Hz, were recorded for each drop test to assess the adequacy of sampling rate to capture the peak impact. For the PC based data acquisition, the peak values of acceleration and pressure upon touchdown are found to be consistent after testing for various sampling frequencies. The time series for acceleration and pressure for a 5.0 m drop with a sampling rate of 1 millisecond is shown in Figure 2. The peak values of acceleration and pressure on touchdown with water surface (0.479 volts and 1.577volts correspondingly) were converted into the acceleration and pressure units after multiplying them with their respective calibration constants. The variation of peak acceleration and impact pressure values derived using different sampling rates are depicted in Figure 3, demonstrating that the peak values of acceleration and pressure remained consistent for a PC based data acquisition for a range of sampling frequencies.

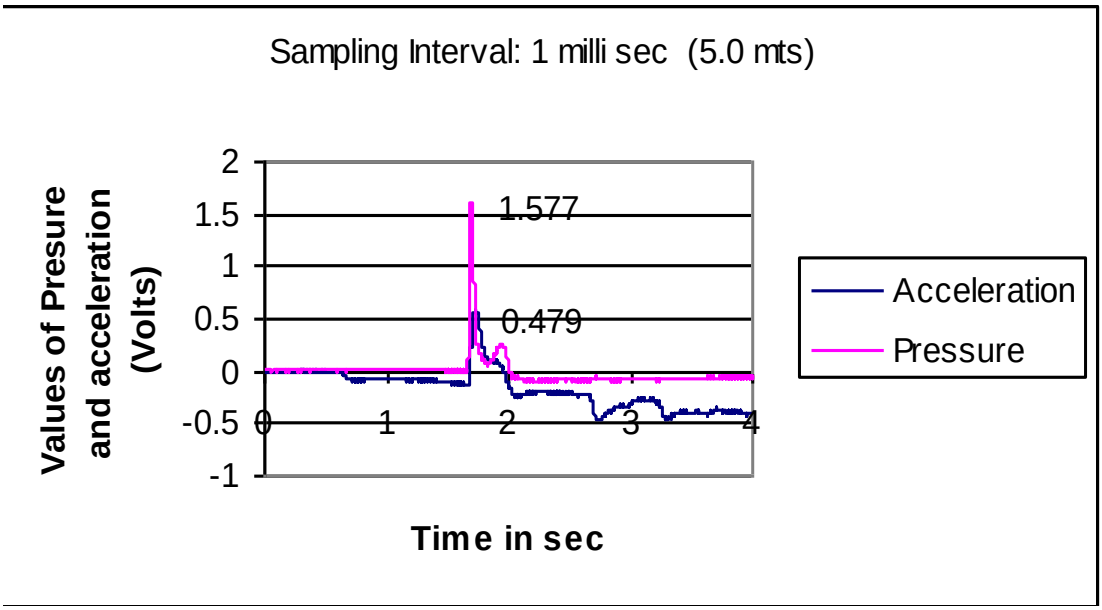

Fig. 2 Acceleration and Pressure Time Histories for a 5m Drop Test
[Maximum impact acceleration = 0.479*11.1*9.91=52.15m/s^2]
[Maximum touchdown pressure = 1.577*0.166=0.26bar]

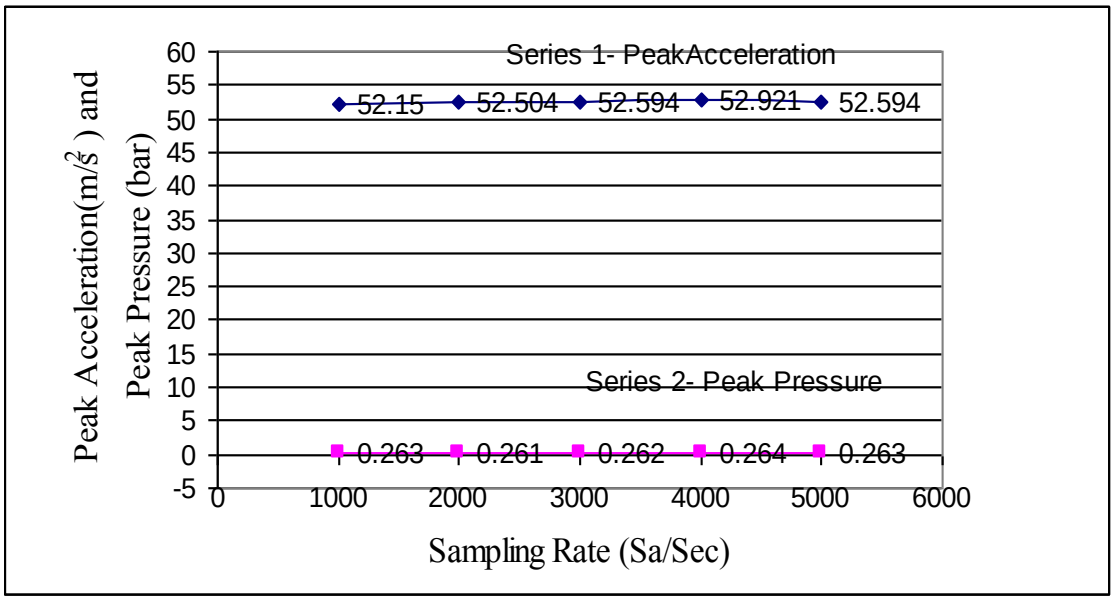

Fig. 3 Peak Acceleration and Peak Pressure vs. Sampling Frequency

Figure 4 depicts the consistency of the peak acceleration and pressure for higher sampling frequencies using an oscilloscope capture (0.01ms to 1.0μs). Since the use of oscilloscope for measurement during the drop tests was impractical, all further tests used only PC based data acquisition to report the peak acceleration and peak pressure upon impact.

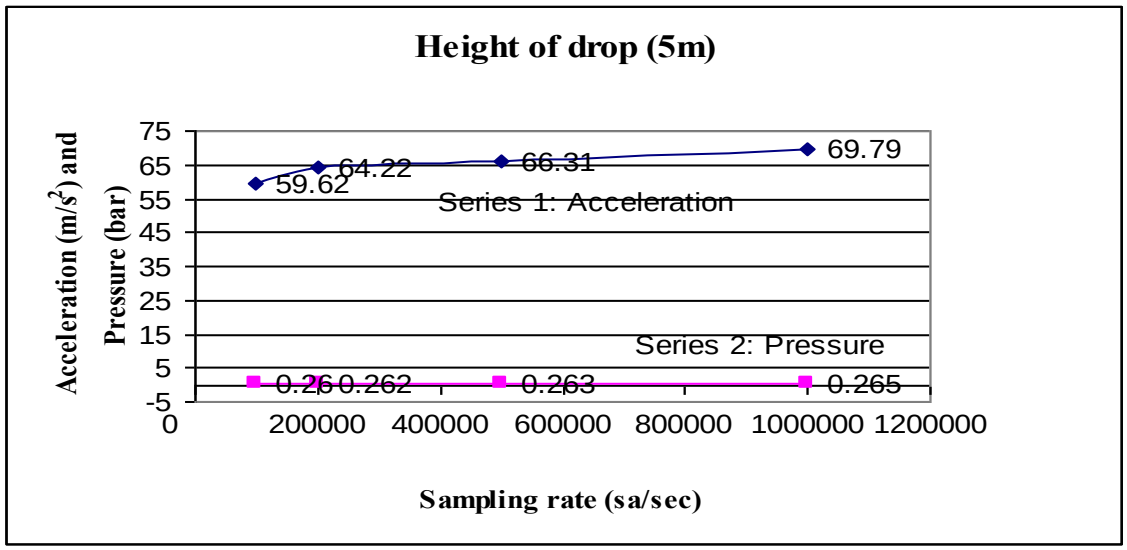

Fig. 4 Peak acceleration and peak pressure vs. sampling rate (Oscilloscope Capture)

Table 2 gives the values of peak pressure, peak acceleration and the estimated force acting on the WLO for drop heights ranging from 1.0 to 5.0m with an increment of 0.5m. The peak value of acceleration for a 5m drop height is 52.170m/s^2 and the peak touchdown pressure is 0.256 bar. The force experienced by the model was obtained using the model mass and measured acceleration (105.9 N for a 5m drop height). While the theoretical velocity was obtained using the height of drop and a g-value of 9.81m/s^2

(by using the kinematic equation of motion), the experimental velocity was obtained by integrating the measured acceleration time history.

Table 2: Results for Drop Test I
[Weight of WLO = 2.03kg (Drop Test I: Ordinary Drop Mechanism)]
(Vertical Entry/Entry Angle=0 deg)

Drop Height (m)	Acceleration (m/s^2)	Pressure (bar)	Force (mass*acc) (N)	Theoretical Velocity (m/s)	Experimental Velocity (m/s)
5.0	52.17	0.25	105.90	9.81	9.79
4.5	48.32	0.23	98.08	9.39	9.27
4.0	45.18	0.22	91.72	8.85	8.61
3.5	38.76	0.19	78.69	8.28	8.26
3.0	37.78	0.18	76.70	7.67	7.55
2.5	33.53	0.16	68.08	7.00	6.87
2.0	30.27	0.15	61.45	6.26	6.20
1.5	22.86	0.13	46.42	5.42	5.31
1.0	11.65	0.12	23.65	4.42	4.39

It can be observed that the impact accelerations and touchdown pressures increase practically linearly with the increase in the height of the drop. Both theory and experiments showed that the peak acceleration was proportional to the square of the impact velocity. There is a practically linear fit between the force and the square of velocity for various drop heights (Kaplan 1968). Comparison of drop heights to theoretical and experimental velocities showed a very good comparison between both the theoretical and experimental velocities ascertaining the accuracy of the impact accelerations measured experimentally for successive drop heights.

2.1.2 Drop Test II

Upon completion of the first set of drop tests presented above, it was decided that a second set of tests with different mass distribution and total weight was warranted. To avoid oscillation of the model during leasing of the cable attachment observed in the first set and achieve better control on the point of release, an electromagnetic release mechanism was designed and implemented. Specifically, a custom designed measuring mechanism on board the WLO enabled the automatic transfer of data in real time to a host computer by means of thin wires. The mechanism along with the steel plate (2mm thick) were glued to the top of the model. The weight of the WLO was increased to 3.5kg. Figure 5 shows the block diagram of the instrumentation setup and all the instruments onboard the WLO.

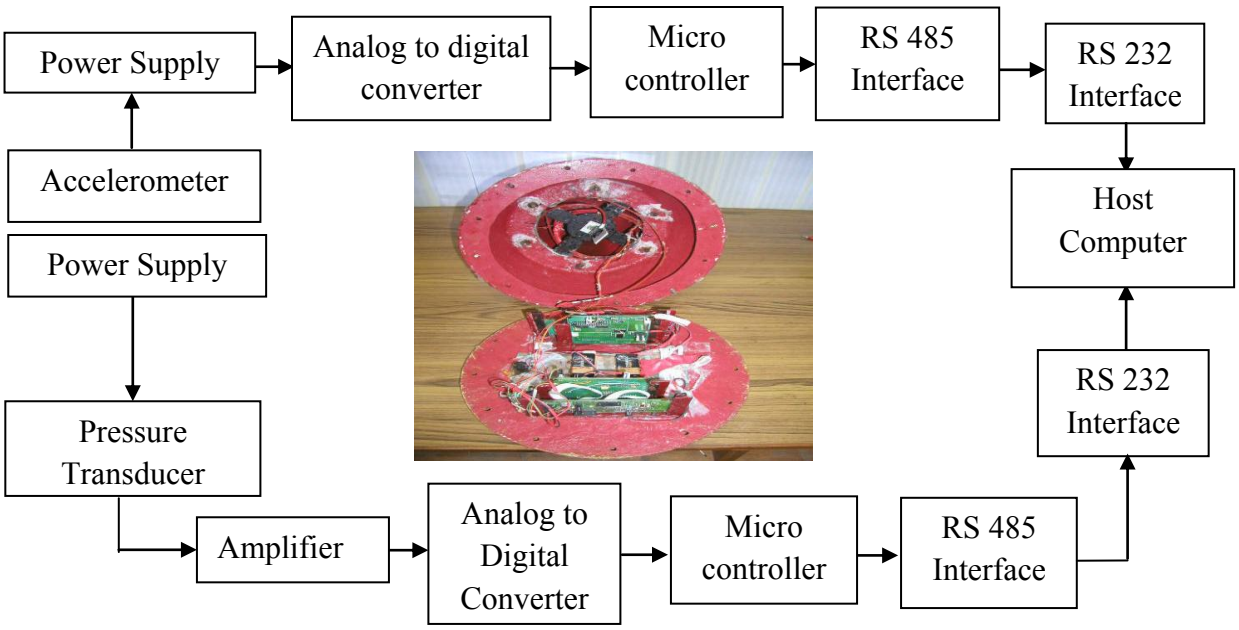

Fig. 5 Block Diagram of the Instrumentation Setup for Drop Test II (Electromagnetic release mechanism)

A steel frame (fabricated in the form of a ladder) was installed on the bridge of the wave basin to hold the electromagnet in position over the water surface. A movable strut was fixed to the steel frame in order to drop the model from every 0.5m height. The electromagnet was bolted at one end of the strut which would hold the model in position. A switch mechanism, provided on the outer surface of the cap of WLO, activated the data recording just before actuating the release. An up-close view of the setup for Drop Test II is shown in Figure 6.

Fig. 6 Up-close view of electromagnet with protruding strut

Pressure and acceleration measurements were obtained using built-in amplifiers connected to a computer through a RS485 link. A single axis MEMS-based accelerometer was used to measure the acceleration and a 5-bar strain gauge-type pressure transducer (mounted at the nose tip) measured the touchdown pressure during impact. The accelerometer and the pressure transducer were connected to amplifiers and a PC based data acquisition system was employed to acquire the data in real time.

The WLO was dropped using the electromagnetic release from the frame fixed to the bridge. The WLO touchdown with the water surface is shown in Figure 7. The model was tested initially for a 0.5m drop and then the height was gradually increased to 5m in steps of 0.5m. The release switch was activated once the model was held to the electromagnet and the acceleration and the pressure data were recorded during the descent. The acceleration and pressure time histories for the single case of a 5m drop, after analysis in the host computer, are shown in Figures 8(a) and 8(b).

Fig. 7 Up-close view of WLO water impact

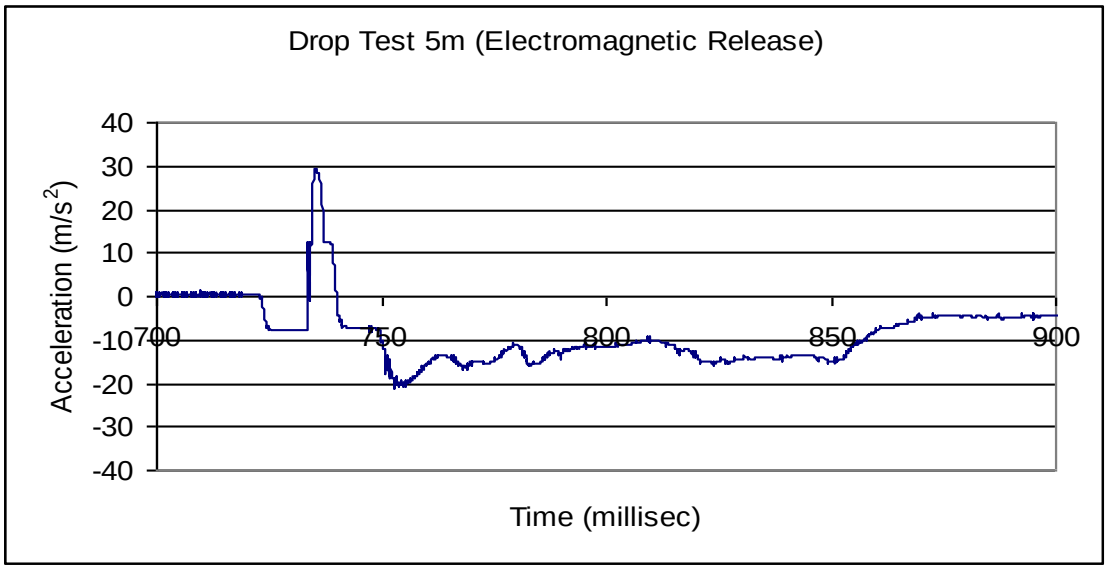

Fig. 8(a) Acceleration time history for a 5m drop test (electromagnetic release)

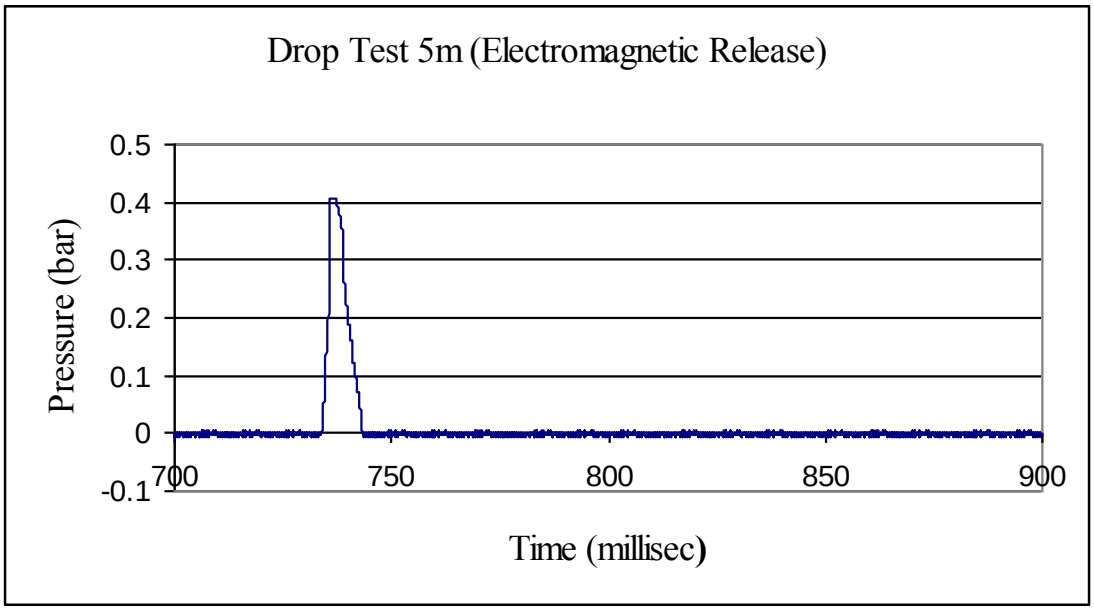

Fig. 8(b) Pressure time history for a 5m drop test (electromagnetic release)

Table 3 gives the values of peak pressure, peak acceleration and the estimated force acting on the WLO for drop heights ranging from 1.0 to 5.0m at an increment of 0.5m. Note that the peak value of acceleration for a 5.0m drop height is 36.501m/s^2 and the touchdown pressure is 0.41bar. The force experienced by the model was obtained using the model mass and measured acceleration (127.725 N for a 5m drop height). While the theoretical velocity was obtained based on drop height and a g-value of 9.81m/s^2, the experimental velocity in the last column was obtained by integrating the measured acceleration time history. As observed in the first drop test, both the peak acceleration and touchdown pressure increases linearly with the increase in the height of drop. The variation of impact force and the square of the velocity depicts that there is a practically linear relationship between the force and the square of velocity for various drop heights,

confirming the results of Kaplan (1968). The accuracy of the experimental measurements was ascertained by the very good comparison between the theoretical and experimental velocities for various drop heights shown in Table 3.

Table 3: Results for Drop Test II
[Weight of WLO = 3.5kg (Drop Test II Electromagnetic Release)]
(Vertical Entry/Entry Angle=0 deg)

Drop Height (m)	Acceleration (bar)	Pressure (m/s^2)	Force (mass*acc) (N)	Theoretical Velocity (m/s)	Experimental Velocity (m/s)
5.0	36.50	0.41	127.72	9.81	9.72
4.5	31.72	0.38	111.02	9.39	9.30
4.0	27.32	0.32	95.62	8.85	8.81
3.5	22.82	0.29	79.87	8.28	8.19
3.0	19.55	0.25	68.42	7.67	7.54
2.5	15.32	0.21	53.62	7.00	6.97
2.0	12.12	0.19	42.35	6.26	6.22
1.5	10.72	0.18	37.52	5.42	5.35
1.0	9.92	0.15	20.22	4.42	4.42

3 Approximate Closed Form Solutions for maximum impact accelerations

For a Water Landing Object (WLO) that has a spherical bottom and is assumed rigid, closed form solutions based on the von Karman and Wagner approaches are available for correlating with the results from the experimental analysis (Wang and Lyle, 2007). The von Karman approach is based on conservation of momentum and uses an added mass. The penetration depth is determined without considering water splash-up. The Wagner approach uses a more rigorous fluid dynamic formulation and considers the effect of water splash-up on the impact force. The kinematic free surface condition was used to determine the intersection between the free surface and the body in the outer flow domain. Satisfaction of the kinematic free surface condition implies that the displaced fluid mass by the body is properly accounted for as rise up of the water. This is not true for a von Karman approach that does not account for the local rise up of the water. From the analytical solutions for a spherical bottom body impacting with water using the von Karman method, the magnitude of the virtual mass for a spherical bottom body is

$$m_v = \frac{4}{3}\rho h^{\frac{3}{2}}(2R-h)^{\frac{3}{2}} \tag{1}$$

where m_v is the virtual mass, ρ is the mass density of water, h is the water depth, and R is the radius of the spherical bottom. The instantaneous velocity, V, of the centre of gravity of the rigid body is

$$V = \frac{db}{dt} = V_0(1+\frac{mg}{W})^{-1} \tag{2}$$

where t is time after impact, V_0 is the initial velocity, g is the gravitational constant, and W is the weight of the rigid body. By substituting Eq. 1 into Eq. 2, the instantaneous velocity can be rewritten as

$$V = \frac{Vo}{1+\frac{8\rho g R^3}{3W}\left(\frac{h}{R}\right)^{\frac{3}{2}}} \tag{3}$$

The overall acceleration, a, can be written as

$$a = \frac{d^2h}{dt^2} = \left[\frac{3\times 2^{\frac{1}{2}}\left(\frac{3W}{4\pi\rho g R^3}\right)^2\left(\frac{V_0^{\,2}}{gR}\right)\left(\frac{h}{R}\right)^{\frac{1}{2}}}{\pi\left(\left(\frac{3W}{4\pi\rho g R^3}\right)+2^{\frac{3}{2}}\pi^{-1}\left(\frac{h}{R}\right)^{\frac{3}{2}}\right)^3}\right] g \tag{4}$$

Assuming $\frac{h}{R}$<<1, the maximum acceleration can be found as

$$a_{\max} = -\frac{256}{243}\left(\frac{4\rho g R^3}{3W}\right)^{\frac{2}{3}}\left(\frac{V_0^{\,2}}{R}\right) \tag{5}$$

with the impact time at

$$t_{\max} = \frac{21}{160}\left(\frac{3W}{4\rho g R^3}\right)^{\frac{2}{3}}\frac{R}{V_0} \tag{6}$$

and the penetration depth at

$$b_{\max} = \frac{1}{8}\left(\frac{3W}{4\rho g R^3}\right)^{\frac{2}{3}} R \tag{7}$$

In the von Karman approach, the rise of water due to the splash up is not considered. The effect of splash up was considered by Wagner and found to have significant effect on the impact force. Recently, Miloh (1991) used a semi-Wagner approach to determine the non-dimensional slamming coefficient that is defined as

$$C_s(\frac{h}{R}) = \frac{2F}{\rho\pi R^2 V_0^2} \tag{8}$$

where F is the impact force. Based on the analytical derivations, Miloh proposed that

$$C_s(\frac{h}{R}) = 5.5(\frac{h}{R})^{\frac{1}{2}} - 4.19(\frac{h}{R}) - 4.26(\frac{h}{R})^{\frac{3}{2}} \tag{9}$$

is suitable for initial stage slamming. Note the coefficients in equation (9) are determined from a set of experimental data from the ACM tests. Based on these analytical derivations the maximum acceleration can be estimated as

$$a^*_{\max} = \frac{g}{2W} C_s\left(\frac{h_{\max}}{R}\right)\rho\pi R^2 V_0^{\,2} \tag{10}$$

Table 4 shows the comparison of the experimental results with analytical solutions. The maximum z-accelerations for a vertical entry for both the drop mechanisms is compared to the closed form solutions based on von Karman and Wagner approaches.

Table 4: Analytical solution results from von Karman and Wagner approaches

Water Landing Object (WLO) Drop Test Cases **Cone radius: 0.0848m** **Max. Radius: 0.3385m**	**Maximum acceleration (Experiments) g: acceleration due to gravity ($\frac{m}{s^2}$)**	**Analytical Solutions for maximum accelerations**		**Equivalent Radius (m) of WLO conical portion**	
		von Karman (Eq.5) a_{max}	**Wagner (Eq. 10)** a^*_{max}	**von Karman** r_{max}	**Wagner** r^*_{max}
Drop Test I: Ordinary drop mechanism	5.2g	14.7g	19.8g	0.0300 m	0.1075 m
Drop Test II: Electromagnetic release mechanism	3.6g	10.4g	25.2g	0.0293 m	0.1310 m

It is important to note that the maximum radius of the base (for a $1/6^{th}$ Froude-scale model of a WLO) is 338.5mm and the radius of the conical portion impacting the water surface is 84.8mm. For a WLO model with the dimensions shown in Table 1, the accelerations obtained from both von Karman and Wagner approaches for experimental Drop Test I are 14.7g and 19.8g, respectively (see Table 4). Similarly, the maximum impact accelerations obtained from both the approaches for Drop Test II are 10.4g and 25.2g, respectively.

Figures 9 and 10 show the values of maximum impact accelerations plotted against the experimental velocity of impact for both the experimental cases and those obtained using the analytical solutions.

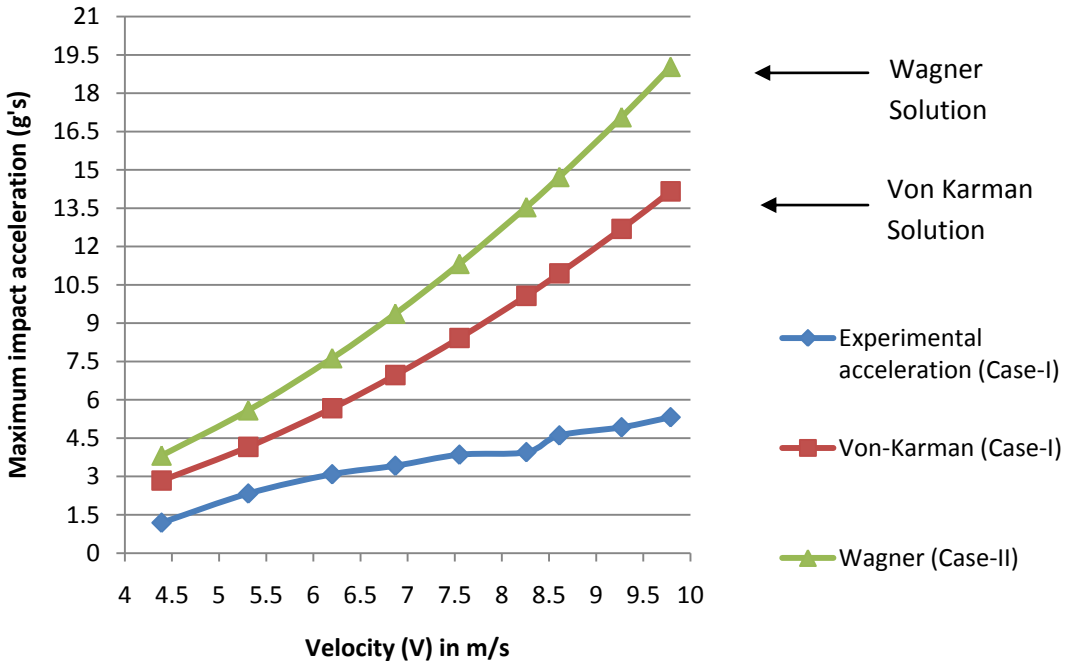

Fig. 9 Maximum acceleration using von-Karman and Wagner solutions (Drop Test I)

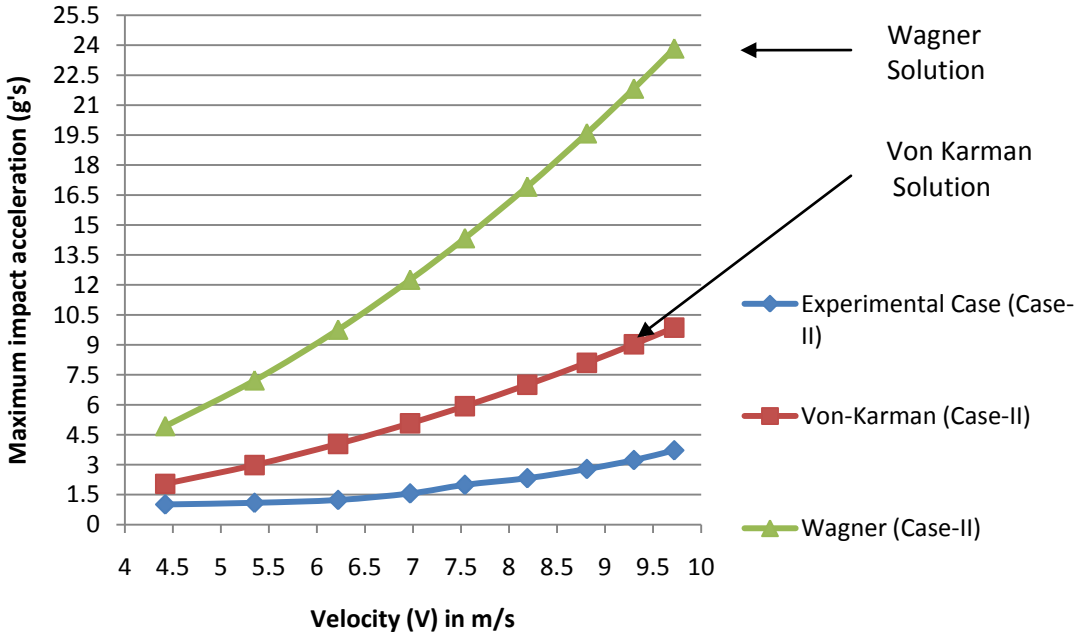

Fig. 10 Maximum acceleration using von-Karman and Wagner solutions (Drop Test II)

For a conical bottomed rigid object, the analytical results show that there is large difference between the experimental peak impact accelerations and those obtained by von Karman and Wagner analytical estimates. The large difference can be attributed to the conical shape of WLO bottom impacting the water surface compared to the large spherical bottom used in deriving the closed form solutions. It can be deduced from Table 4 that for a conical bottomed rigid object (like the WLO), the experimental values of peak impact accelerations (for a 0-degree pitch), do not fit in the bounds on maximum impact accelerations calculated by both von Karman and Wagner approaches.

In addition to the unique shape of the WLO (which is primarily responsible for the large deviation of the experimental impact accelerations from the closed form solutions) the basic assumptions of the formulations for both von Karman and Wagner approaches also play a pivotal role in contributing to the large difference. The von Karman approach is based on conservation of momentum (using an added mass) and the penetration depth is determined without considering water splash-up, thus neglecting the highly nonlinear coupled fluid-structure interaction effect. The Wagner approach, on the other hand, attempts to relax the von Karman no-splashing assumption by using a rigorous dynamic formulation and incorporates the effect of the upward splashing of the water and its effects on the motion of the object. With the upward splashing correction, the Wagner approach tends to over predict the maximum impact retardation as it neglects water compressibility (i.e. a more yielding fluid) near the impact zone.

The lack of agreement in the peak acceleration obtained in the present experimental study with the closed form von Karman and Wagner approximate solutions is due to the

large initial angle at impact and the relatively rapid changes in contact radius of the inverted cone shape of the WLO as it penetrates the water surface. These deviations from the idealized assumption may be taken into account using the concept of an equivalent radius.

3.1 An equivalent radius approximate semi-analytical procedure

In order to capture the proper modeling of the dynamics of the impact and to ascertain a true fluid behavior, an attempt was made to calculate an equivalent radius of the conical portion of the WLO that would compare well with the experimental impact acceleration. The values of the equivalent radius of WLO using von Karman and Wagner approaches for both drop tests are shown in Figure 11 and summarized in Table 4.

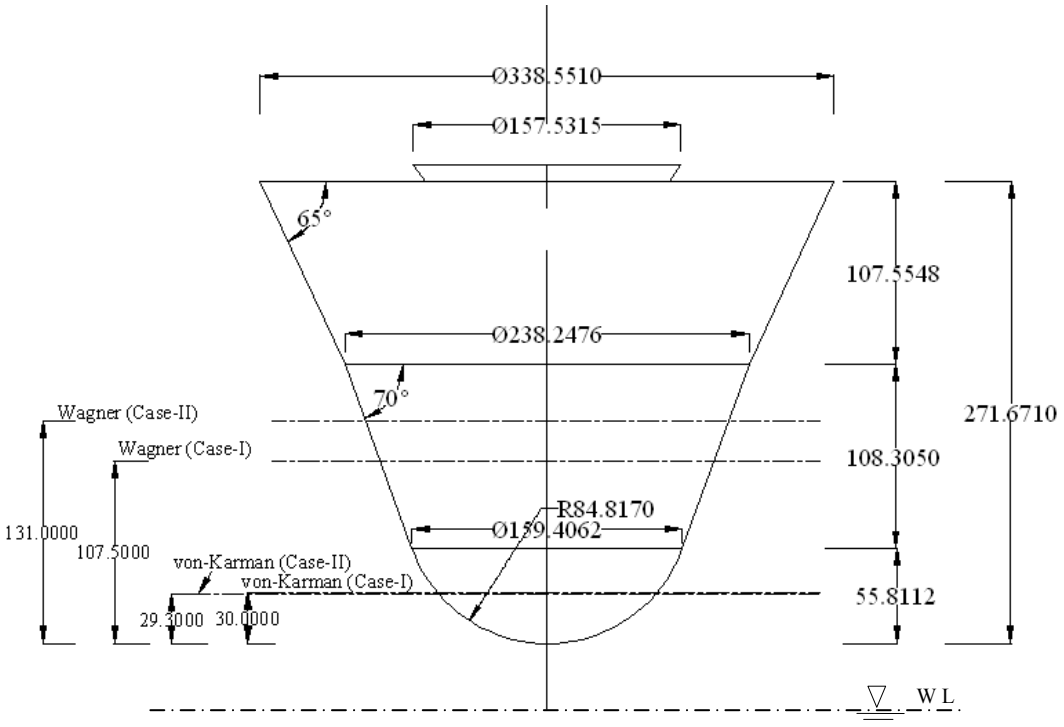

Fig. 11 Equivalent radius of the WLO model

From the von Karman approach the equivalent radius for Drop Test I and II are 30.0 mm and 29.3 mm, respectively. It can be observed that the von Karman approach tends to estimate a lower value of the radius of the conical portion. As the effect of local rise up of the water is significant during water entry of a rigid 3D object, the von Karman predictions for maximum impact accelerations are not significant in determining the maximum impact accelerations for the water entry of WLO. The Wagner approach on the other hand estimates the equivalent radius for Drop Test I and Drop Test II as 107.5mm and 131mm, respectively.

Based on the equivalent radius approach, approximate semi-analytical solutions based on the von Karman and Wagner theories can be used to obtain design maximum accelerations of the WLO model consistent with experimental results.

In order to further comprehend the effect of the shape of the object (especially the conical portion of the WLO impacting the water surface first), the values of equivalent radius (r) are plotted against different velocities of impact for both Drop Test I and II (Figures 12). The equivalent radius (r) was initially obtained for each drop velocity for both the experimental cases. The idea is to obtain those values of the radii which would give the same experimental impact accelerations corresponding to the impact velocities. Observe that from Figure 12 the values of equivalent radius (r) of the WLO model remain almost constant for different velocities of impact for both cases.

The next step is to compare the accelerations obtained experimentally (Drop Test I and II) to those obtained by using a mean equivalent radius (r*). The values of r* were

obtained by taking the mean of all the equivalent radii obtained for different impact velocities corresponding to their respective impact accelerations. For each r* obtained for each case, the impact accelerations were calculated by varying the impact velocity. Figure 13 shows the comparison for the maximum impact accelerations and those obtained by the mean equivalent radius (r*).

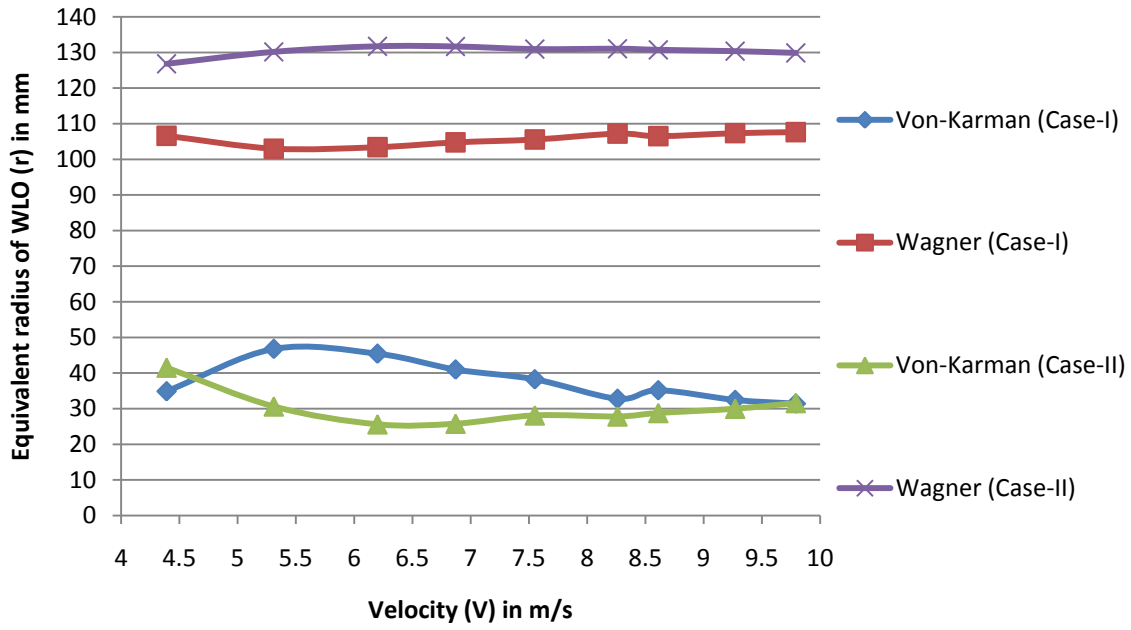

Fig. 12 Equivalent radius (r) of the WLO for different velocities of impact for Drop Test I and II using von-Karman and Wagner approaches

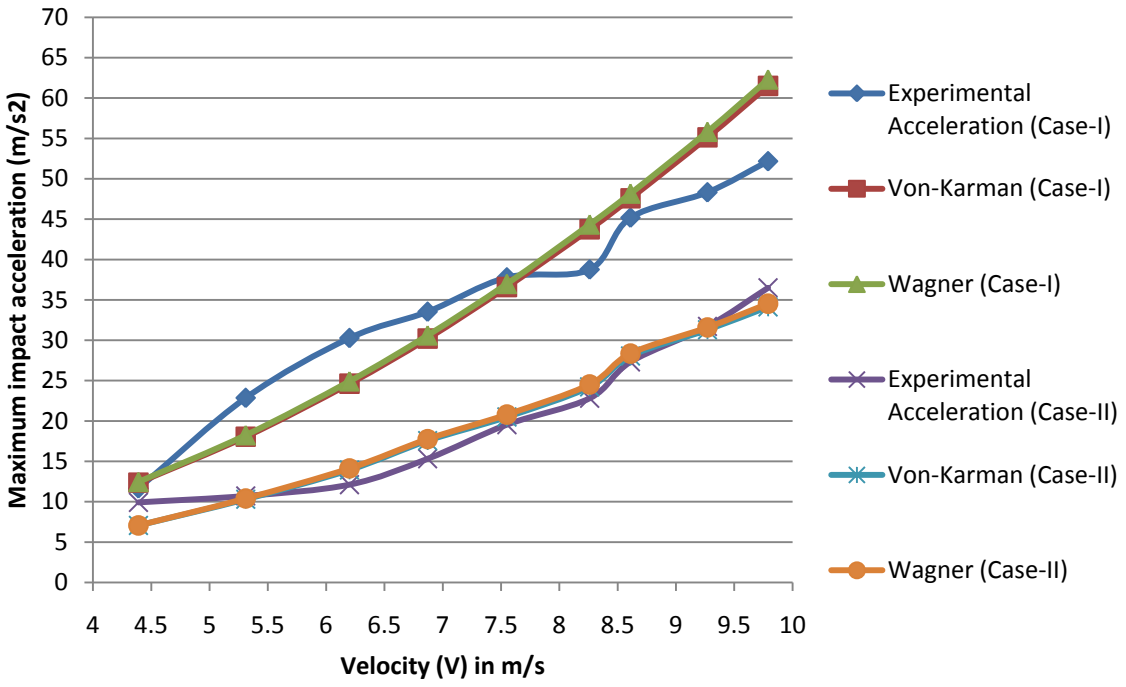

Fig. 13 Mean equivalent radius (r*) of the WLO for different velocities of impact for Drop Test I and II using von-Karman and Wagner approaches

Figure 13 shows that the maximum impact accelerations obtained by both the semi-analytical models seem to compare reasonably well with the experimental peak impact accelerations. It is interesting to note that the acceleration values obtained by von Karman and Wagner solutions produce accelerations that are similar ascertaining the importance of the shape of the WLO during water impact. (Note that we call the proposed approximate estimation procedure semi-analytical because experimental data is needed to determine an important parameter, namely, the equivalent radius.)

4 Discussion and Comparison

An important aspect is the comparison of the shape of space capsule used for the Indian and American space missions. The WLO used for the Indian space mission is conical in shape with a rounded nose than compared to the convex shape of the base used for all the American space missions. This significantly inhibits the comparison with the literature available for ACM or other American space missions. The present work is the first of its kind in testing a scaled-down model of WLO (with a conical shaped base) impacting ocean waters. However, the results obtained from the WLO experiments can be used to qualitatively justify the impact accelerations and touchdown pressures coming on to the object.

For the WLO weighing 2.03kg (Drop Test I), the acceleration time series for a 10m/s velocity of impact gives a peak acceleration of 52.17 m/s^2 (~5.2 g) and a touchdown pressure of 0.25bar and for the WLO tests with the electromagnetic release with an increased mass of 3.5kg of the model (Drop Test II), the peak acceleration was found to be 36.5 m/s^2 (~3.6 g) and the touchdown pressure was computed as 0.49bar. In addition, for both independent experimental data sets, the peak force was proportional to the square of the impact velocity, which is in good agreement with Kaplan‟s theoretical results. Hence, a formal comparison between the two cases cannot qualitatively demonstrate the efficiency of one case over the other. Instead, for an end user, an increased weight of WLO provides a measure of the reduction of the accelerations (3.6 g in Drop Test II compared to 5.2 g in Drop Test I).

The peak impact force experienced by the model obtained using the model mass and measured acceleration is 105.9 N for Drop Test I compared to 127.725 N for Drop Test II. Comparison of drop heights to theoretical and experimental velocities depict a very good agreement for both the cases, ascertaining the accuracy of the impact accelerations measured experimentally for successive drop heights.

In order to describe the physics of the slamming problem, the maximum pressure obtained was compared to the pressure calculation when a circular cylinder slams water surface (Faltinsen 1990). The maximum pressure for both cases was well below the pressure bound ($\rho c_e V$). Interestingly, the horizontal component of velocity was found to have a very little effect on the accelerations in the vertical (Z) direction in both drop tests. No effort was made to measure neither the horizontal component of velocity nor the entry angle was varied.

The WLO was assumed as rigid for the convenience of comparing experimental results with closed form solutions for maximum accelerations predicted by the classical von Karman and Wagner. The maximum radius of the base of the model is 338.5mm whereas the radius of the conical portion impacting the water surface is 84.8mm which is primarily responsible for the large difference between experimental and analytical estimates. An improved approximate solution procedure using an “equivalent” radius concept integrating experimental results with the von Karman and Wagner closed-form solutions is proposed and developed in detail.

5 Concluding Remarks

An important aspect in the assessment of recovery and escape systems is the performance of such objects in ocean water landing. The primary objective is to study the dynamics of a WLO during water impact by performing experiments using a $1/6^{th}$ Froude-scale model of a using two independent drop mechanisms. Drop Test I involved dropping the object using a rope and pulley arrangement, while Drop Test II employed an electromagnetic release to drop the object. The effects of varying the vertical velocity and the WLO weight are identified and the trend obtained helps the readers to comprehend the conditions that must be avoided during a water impact.

The hydrodynamic parameters such as peak acceleration, touchdown pressure and maximum impact force were measured and the dynamics during the touchdown of WLO was observed. The peak values of acceleration for Drop Test I and II are $5.2\,g$ and $3.6\,g$, respectively. If a crew member onboard the WLO cannot withstand impact accelerations over $5\,g$, these results will give a glimpse of the initial conditions which will keep the peak impact accelerations under the specified limits

An important aspect is the accuracy and reliability of the experimental results in predicting the impact accelerations and touchdown pressures obtained from both the experimental cases. Results from both the experimental data sets show that the impact acceleration and touchdown pressure increases practically linearly with the increase in the height of the drop.

The reliability of the experimentally measured maximum accelerations was calibrated with classical von Karman and Wagner approximate closed-form solutions. For a conical bottomed rigid object, the analytical results show that there is a large difference between the experimental peak impact accelerations and those obtained by these analytical estimates. The large difference can be partly attributed to the unique shape of the WLO and partly due to the assumptions of the formulations for both von Karman and Wagner approaches. Owing to the large difference between the experimental accelerations and those provided by von Karman and Wagner approaches, an improved approximate solution procedure using an "equivalent" radius (r) of the WLO was estimated to understand the physics of the impact. It can be observed that the von Karman approach tends to estimate a lower value of the radius of the conical portion whereas the Wagner approach tends to estimate a higher value of the impact radius.

As the effect of local rise up of the water is significant during water entry of a rigid 3D object, the von Karman predictions for maximum impact accelerations are not significant in determining the maximum impact accelerations for the water entry of WLO. Based on the equivalent radius approach, the approximate analytical solutions of von Karman and Wagner can be used to obtain design maximum accelerations of the WLO model consistent with experimental results. Further, the mean equivalent radius (r*) was computed to analytically estimate the maximum impact accelerations (for varying impact velocities). Results show the maximum impact accelerations obtained by both the semi-analytical estimates compared reasonable well with the experimental acceleration values.

In order to achieve accelerations comparable to the closed-form solutions, the analytical results show that, for the design of a WLO, the Wagner approach provides a correct estimate of the equivalent radius of the WLO. It is, however, interesting to note that the acceleration values obtained by von Karman and Wagner solutions produce accelerations that are similar ascertaining the importance of the shape of the WLO during water impact.

Finally, several areas are worthy of mention at this juncture. Model testing is needed over a wider range of conditions to include improved tests which vary the speed, weight and entry angle and under realistic conditions existing in the oceans. The model used for the drop tests should be specifically designed to avoid structural vibrations.

Future work can also include more in-depth analysis of the vehicle impact pressures, fully deformable vehicles and floatation studies. Numerical simulations of the WLO splashdown can be performed and the possibility of combining the finite element package with a computational fluid dynamics package could more accurately simulate the hydrodynamics during impact.

Acknowledgements

The authors gratefully acknowledge the valuable comments and suggestions by the conference papers reviewers and discussions with experts in the area especially Professor Odd Faltinsen. Financial support from the US Office of Naval Research Grants N00014-10-10230 and N00014-11-10094, and the National Science Foundation

Grants CMS-0217744 and CMS-0530759 for the first and second authors is gratefully acknowledged.

References

Baker, E., and Westine, S., 1967. "Model tests for structural response of Apollo Command Module to water impact," *Journal of Spacecraft and Rockets*, **4**(2), pp. 201-208.

Brebbia, C.A., and Nurick, G.N., 2003. "Advanced in Dynamics and Impact Mechanics," WIT Press.

Faltisen, O. M., 1990. "Sea loads on ships and offshore structures," Cambridge University Press, Cambridge.

Faltinsen, O. M., and Zhao, R., 1997. "Water entry of ship sections and axisymmetric bodies," *AGARD FDP Workshop on High Speed Body Motion in Water held in Kiev, Ukraine, 1-3 September.*

Hirano, Y., and Miura, K., 1970. "Water impact accelerations of axially symmetric bodies," *Journal of Spacecraft Rockets*, **7**(6), pp. 762-764.

Kaplan, A., 1968. "Simplified dynamic analysis of Apollo water impact, including effects of the flexible heat shield," 11176-11176-6004-R0-00, TRW, Redondo Beach, California, USA.

Korobkin, A. A., 2004. "Analytical models of water impact," *European Journal of Applied Mathematics*, **15**, pp. 821-838.

Korobkin, A. A., and Scolan, Y. M., 2006. "Three-dimensional theory of water impact.

Part 2. Linearized Wagner problem," *Journal of Fluid Mechanics*, **549**, pp. 343-373.

Miloh, T., 1991. "On the initial-stage slamming of a rigid sphere in a vertical water entry," *Applied Ocean Research*, **13**(1), pp. 43-48.

Scolan, Y. M., and Korobkin, A. A., 2001. "Three-dimensional theory of water impact. Part 1. Inverse Wagner problem," *Journal of Fluid Mechanics*, **440**, pp. 293-326.

Seddon, C. M., and Moatamedi, M., 2006. "Review of water entry with applications to aerospace structures," *International Journal of Impact Engineering*, **32**, pp. 1045-1067.

Wang, J. T., and Lyle, K. H., 2007. "Simulating space capsule water landing with explicit finite element method," 48th AIAA/ASME Conference, April, pp. 23-26, Waikiki, HI, USA.

Wierzbicki, T., and Yue, D. K., 1986. "Impact damage of the challenger crew compartment," *Journal of Spacecraft and rockets,* **23**, pp. 646-654.

Wriggers, P., and Nackenhorst, U., 2005. "Analysis and Simulation of Contact Problems," Springer

Zhao, R., and Faltinsen, O., 1993. "Water entry of two-dimensional bodies," Journal of Fluid Mechanics, 246, pp. 593-612.

Chapter 3

Rigid-Object Water-Entry Impact Dynamics: Finite-Element/Smoothed Particle Hydrodynamics Modeling and Experimental Calibration

Rigid-Object Water-Entry Impact Dynamics: Finite-Element/Smoothed Particle Hydrodynamics Modeling and Experimental Calibration

Ravi Challa[1], Solomon C. Yim[2], V.G. Idichandy[3] and C.P. Vendhan[3]

[1]Graduate Student, School of Civil and Construction Engineering, Oregon State University, Corvallis, OR- 97330
[2]Professor, Coastal and Ocean Engineering Program, School of Civil and Construction Engineering, Oregon State University, Corvallis, OR-97330
[3]Professor, Department of Ocean Engineering, Indian Institute of Technology Madras, Chennai-600036

The contents of this paper are based on two articles (OMAE-10-20658 and OMAE-10-20659) presented at the 29th International OOAE Conference in Shanghai, China. Significant revisions and improvements have been made incorporating comments and suggestions from reviewers and discussions with expert researchers at and after the conference presentations.

Abstract

A numerical study on the dynamic response of a generic rigid water-landing object (WLO) during water impact is presented in this paper. The effect of this impact is often prominent in the design phase of the re-entry project to determine the maximum force for material strength determination to ensure structural and equipment integrity, human safety and comfort. The predictive capability of the explicit finite-element arbitrary Lagrangian-Eulerian (ALE) and smoothed particle hydrodynamics (SPH) methods of a state-of-the-art nonlinear dynamic finite-element code for simulation of coupled dynamic fluid structure interaction (FSI) responses of the splashdown event of a WLO were evaluated. The numerical predictions are first validated with experimental data for maximum impact accelerations and then used to supplement experimental drop tests to

establish trends over a wide range of conditions including variations in vertical velocity, entry angle and object weight. The numerical results show that the fully coupled FSI models can capture the water-impact response accurately for all range of drop tests considered and the impact accelerations are practically linearly with the increase in the height of the drop. The WLO was assumed as rigid, so the numerical results could be correlated with closed form semi-analytical solutions. In view of the good comparison between the experimental and numerical simulations, both the models can readily be employed for parametric studies and for studying the prototype splashdown under more realistic conditions existing in the oceans.

1 Introduction

The ocean entry dynamics of a generic WLO is an intrinsic component of many naval applications. The present study is concerned with the numerical analysis of the ocean water landing of a generic rigid object (WLO) and its comparison with the experimental results. The effect of this impact is often prominent in the design phase of the re-entry project, to determine the maximum force for material strength determination to ensure structural and equipment integrity and human safety. It is important to determine the maximum force to identify the design alternatives that are within the physical limitations of crew members and materials.

Prototype data (generic shape and dimensions) has been provided by the Indian Space Research Organization (ISRO) to facilitate making a physical model of the WLO. The

shape of the prototype is unique in a way that it is conical with a rounded nose (which impacts the water surface first) than compared to the convex shape of the base used for American space missions. This significantly inhibits the comparison with the literature available for ACM or other American space missions.

Studies on impact phenomena based on the theoretical and experimental work by von Karman (1929) resulted in equations for the impact of rigid bodies on a fluid assuming that the reaction of water was solely due to its inertia. Using an expression for the added mass due to water, the accelerations and pressures affecting the rigid body were determined. Miloh (1991) obtained analytical expressions for the small-time slamming coefficient and wetting factor of a rigid spherical shape in a vertical water entry. A semi-Wagner approach was then used to compute the wetting factor and the Lagrange equations were employed in order to determine the slamming force from the kinetic energy of the fluid. A good agreement between theoretical model and experimental measurements, both for the early-stage impact force and the free-surface rise at the vicinity of the sphere was observed.

Faltinsen (1997) studied the theoretical methods for water entry of two-dimensional and axisymmetric bodies. A numerical method is verified by comparing with the asymptotic method and validated by comparing with experiments for cones and spheres. The significance of the effect of local rise up of the water during entry was presented.

Brooks and Anderson (1994) investigated the dynamic response of water-landing space module (WLSM) during impact upon water. A $1/5^{th}$-scale model was tested in a three-

dimensional (3-D) basin at the Hinsdale Wave Research Laboratory at Oregon State University and the results were compared with those obtained using analytical techniques and computer simulations. The 3-D FE model was validated by comparison with previous full-scale test data and theory.

Scolan and Korobkin (2001) considered the three-dimensional problem of a blunt-body impact onto the free surface of an ideal incompressible liquid based on Wagner‟s theory. Lin et al. (2002) evaluated the performance of ALE formulation. Their work predicted that the current scalability of the numerical code though capable in making the code run faster, is inadequate for robust FSI applications. Olovsson and Souli (2002) evaluated the capabilities of FSI and ALE formulation for various fluid dynamics problems and they showed that FE code is an efficient tool for analyzing large deformation processes with its multi-material ALE capabilities. Tutt and Taylor (2003) assessed the performance of recovery vehicles in the event of a water landing. They investigated the application of the Eulerian-Lagrangian penalty coupling algorithm and multi-material ALE capabilities for the water impact. Melis and Khanh Bui (2003) studied the ALE capability to predict splashdown loads on a proposed replacement/upgrade of the hydrazine tanks on the thrust vector control system housed within the aft skirt of a Space Shuttle solid rocket booster. Preliminary studies on the booster impacting water showed that useful predictions can be made by applying the ALE methodology to a detailed analysis of a 26-degree section of the skirt with proposed tank attached. Seddon and Moatamedi (2006) reviewed the work undertaken in the field of water entry between 1929 and 2003, providing a summary of the major theoretical, experimental and

numerical accomplishments in the field. Wang and Lyle (2007) simulated the space capsule water landing using an arbitrary Lagrangian-Eulerian (ALE) finite-element (FE) solver and a penalty coupling method to predict the fluid and structure interaction forces. The capsule was assumed rigid and the results were found to correlate well with close form solutions.

It is apparent that though the FE codes were used for many fluid-structure interaction problems in the past, modeling water behavior in such problems still poses difficulties. A general-purpose non-linear transient dynamic finite element code for analyzing large deformation dynamics response of structures including structures coupled to fluids is used in the present study. The dynamic behavior of the WLO dropped from specific heights (with varying entry speed and weight) to provide data for calibration of prediction results from numerical studies is examined. Subsequently, the experimental and numerical results were correlated with classical solutions using the von Karman and Wagner approaches for maximum impact acceleration.

2 Finite-Element Modeling of the Experimental WLO Drop Tests

The predictive capability of the state-of-the-art nonlinear explicit dynamic finite element code is evaluated. This work utilizes the built-in contact-impact algorithm along with the ALE and SPH features in LS-DYNA to simulate the fully coupled FSI phenomenon.

For the problem considered, the structural response involves the penetration of the object treated essentially as a rigid body through the water domain. The simulation model

involves two components (i) WLO, and (ii) water-void domain. The overall configuration of the WLO prototype is shown in Figure 1. The WLO model has mass of 2.5kg and the maximum height and the maximum base diameter are 271mm and 338mm respectively.

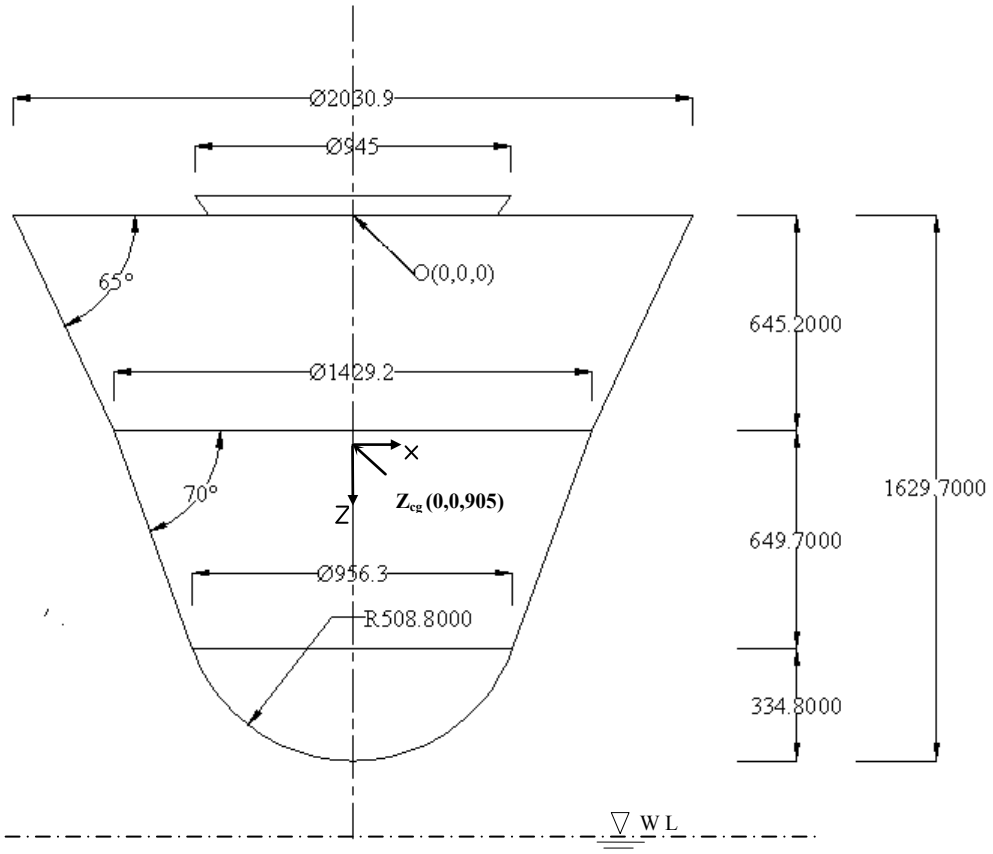

Fig. 1 Overall configuration of WLO Prototype
(All dimensions are in mm)

The water was modeled using solid brick elements. A water body of 4m (diameter) x 2m (length) was chosen for the impact studies. The FE mesh for the void domain had dimensions 4m (diameter) x 0.6m (length) and both the water and void domain was

modeled as a cylindrical mesh. The WLO is treated as a rigid material with a Young‟s modulus of 4.895 X 10^9 N/m^2 (FRP), Poisson ratio of 0.2, and a mass density of 1764.52 kg/m^3 (FRP). Null material model which has very little shear strength to model fluid with a mass density of 1000 kg/m^3 is used for the water domain and an initial vacuum with a zero mass density is used for the void domain.

Eight-node brick elements and 4-node Belytschko-Lin-Tsay shell elements (Hallquist, 1998) are used for discretization of the water domain and WLO, respectively. In the present study, a constrained Lagrange interface/contact is used to model the impact event between the object (treated as a rigid body) and the water-void target. In this, the moving surface of three-dimensional space capsule (a Lagrangian mesh) is treated as the slave surface, and the target water-void mesh is treated as the master surface. Importantly, Navier Stokes equations and ALE formulations are solved all over the computational domain. The ALE differential form of the conservation equations for mass, momentum, and energy are readily obtained from the corresponding Eulerian forms:

Mass: $$\frac{d\rho}{dt} = \left.\frac{\partial \rho}{\partial t}\right|_x + c \cdot \nabla \rho = -\rho \nabla \cdot v \qquad (1)$$

Momentum: $$\rho \frac{dv}{dt} = \rho \left(\left.\frac{\partial v}{\partial t}\right|_x + (c \cdot \nabla) v \right) = \nabla \cdot \sigma + \rho b \qquad (2)$$

Energy: $$\rho \frac{dE}{dt} = \rho \left(\left.\frac{\partial E}{\partial t}\right|_x + c \cdot \nabla E \right) = \nabla \cdot (\sigma \cdot v) + v \cdot \rho b \qquad (3)$$

where ρ is the mass density, v is the material velocity vector, σ denotes the Cauchy stress tensor, F is the specific body force vector, and E is the specific total energy, $\hat{v}$ is the grid velocity, and c is the convective velocity ($c = v - \hat{v}$).

The boundary conditions employed in the numerical model are partially the material surfaces (out-of-plane, in-plane and bending restraint). The material surfaces defined in ALE formulation are: (a) no particles can cross them, and (b) stresses must be continuous across the surfaces. The elements of the water domain were given the null hydrodynamic material type that allowed a new equation of state to be specified. The Gruneisen equation of state with cubic shock velocity-particle velocity is applied in our numerical model and it defines pressure as:

$$p = \frac{\rho_0 C^2 \mu [1 + (1 - \frac{\gamma_0}{2})\mu - \frac{\sigma}{2}\mu^2]}{[1 - (S_1 - 1)\mu - S_2 \frac{\mu^2}{\mu + 1} - S_3 \frac{\mu^3}{(\mu + 1)^2}]} + (\gamma_0 + \alpha\mu)E \tag{4}$$

where E is the internal energy per initial volume, C is the intercept of the $u_s - u_p$ curve. $S_1, S_2,$ and S_3 are the coefficients of the slope of the $u_s - u_p$ curve, γ_0 is the Gruneisen gamma, and α is the first order volume correction to γ_0. (The speed of sound in water was set to 1484m/s with S_1 set to 1.979 and a volume correction factor γ_0 is 0.11.) The edges of the water block were defined as non-reflecting boundaries allowing the water block to be relatively small in size. Termination time of the process and the time step increment is set by the user based on the processing time. This time step size is then

automatically adjusted throughout the transient analysis based on the deformation and stress state of each structural element.

3 Finite-element simulations

Simulations were performed using the software over a wide range of conditions. The characteristics of entry speed, entry angle, and vehicle weight were varied. For each simulation, a total of 2000 data states were created from the simulation. Displacement, velocity and acceleration of the model were recorded at each data dump. An important result from these simulations is the peak acceleration experienced by the object upon impact. Each simulation output has been suitably filtered to remove the „noisy peaks" caused by modeling the otherwise unbounded water domain as a finite one. Figure 2 shows the computational mesh for the water impact analysis. In all the numerical simulations the accelerations are measured in the local Z directions, unless indicated otherwise.

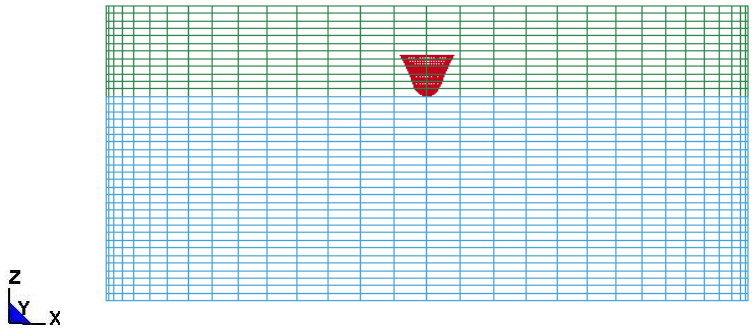

Fig. 2 Computational mesh for water impact analysis
(Blue: Water domain /Green: Void Domain/ Red: WLO model)

Effects of Vertical Velocity Variation --- The vertical velocities of the WLO at impact considered in this numerical study ranged from 10m/s to 4 m/s (with 9.8 m/s corresponds to the maximum scaled down impact velocity upon water landing). Figure 3 shows the unfiltered data of the acceleration time history. It was observed that the unfiltered raw acceleration time history does not give a clear picture of the impact acceleration (noisy peaks); hence, a proper filtering technique need be used to process the data. Similar to the results presented in the Langley Experiments (Anderson, 1994), the simulation data of the acceleration time history was filtered using a low-pass sawtooth filter. Sawtooth filter at 1156Hz yielded results that are remarkably close to the WLO experimental impact data, providing a high degree of confidence in the applicability of ALE methodology to this class of intricate impact problems. For a 5m drop height, Figure 4 shows that the filtered peak acceleration upon impact corresponds to 51.52 m/s^2. Figure 5 shows a linear relationship between the depth of immersion and the drop height. Table 1 shows the comparison of experiments (Case-I: Mechanical release of WLO) with ALE technique.

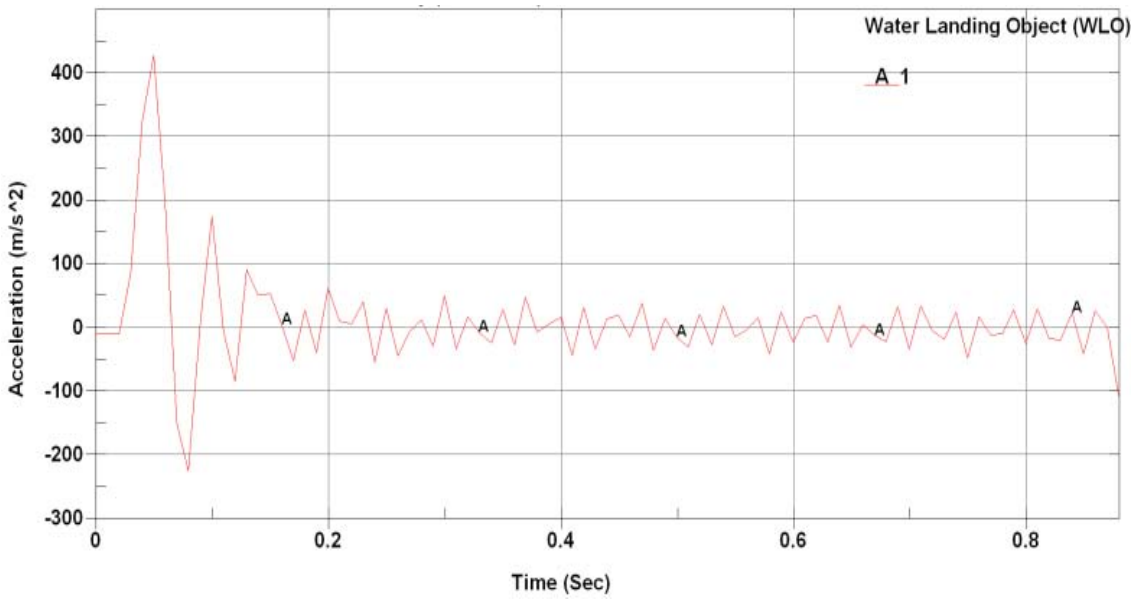

Fig. 3 Acceleration vs. Time for a vertical velocity of 9.81m/s

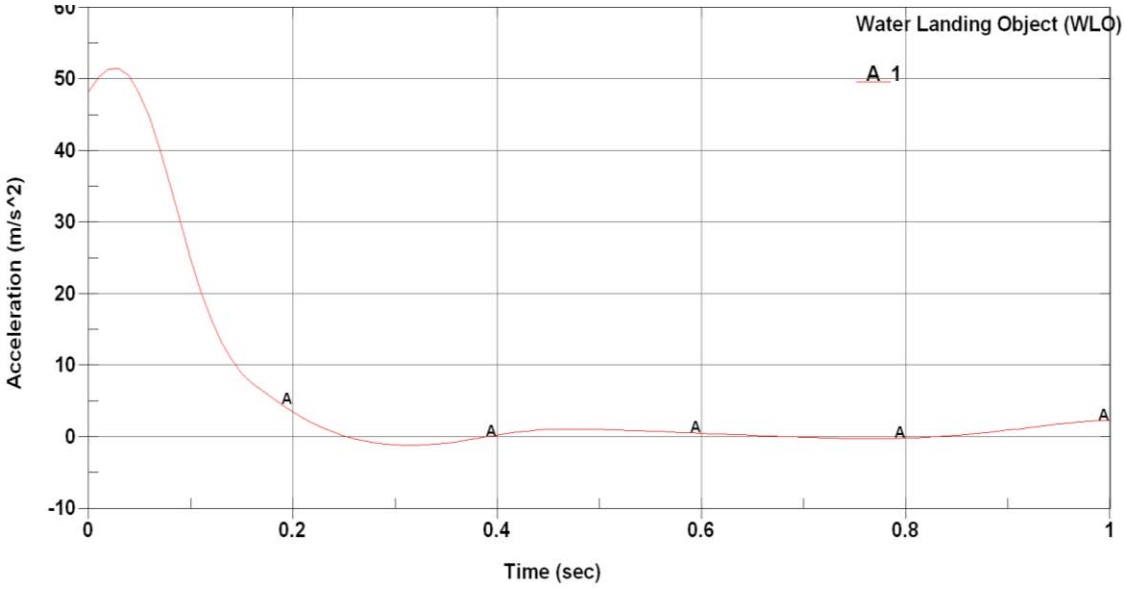

Fig. 4 Filtered Acceleration time history (Sawtooth filter @ 1156Hz)

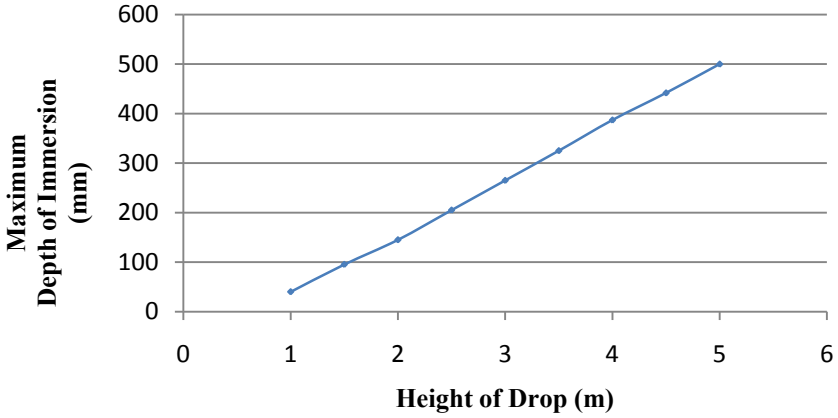

Fig. 5 Height of Drop vs. Depth of Immersion for Case-I

Table 1: Results for maximum acceleration filtered at 1400 Hz [Weight of WLO = 2.03kg (Vertical Entry/Entry Angle=0 deg)]

Vertical Velocity at impact (m/s)	Maximum Acceleration (Numerical) (m/s^2)	Maximum Acceleration (Experimental) (m/s^2)	Percent Deviation (%)
9.81	51.52	52.71	2.25
9.2	50.78	51.61	1.60
8.6	44.21	45.18	2.16
8.2	37.80	38.76	2.47
7.5	36.41	37.78	3.62
6.8	32.15	33.53	4.56
6.2	29.01	30.27	4.16
5.3	21.74	22.86	4.89
4.3	10.95	11.65	6.0

Effects of Entry Angle Variation --- The entry angles of the WLO upon impact were varied from 15 to 30 deg (Table 2) to examine its influence on peak acceleration. These simulations show that the impact acceleration can be reduced by having the WLO enter the water at an angle. Figure 6 shows the animation images at various time steps. These fluid density plots show the fringe levels at various stages of penetration successfully demonstrating the ALE features for the impact problem. Figure 7 displays the raw unfiltered acceleration time history data for a 15 deg entry angle. Filtered acceleration time series (Figure 8) yields a peak acceleration value of 41.08m/s^2.

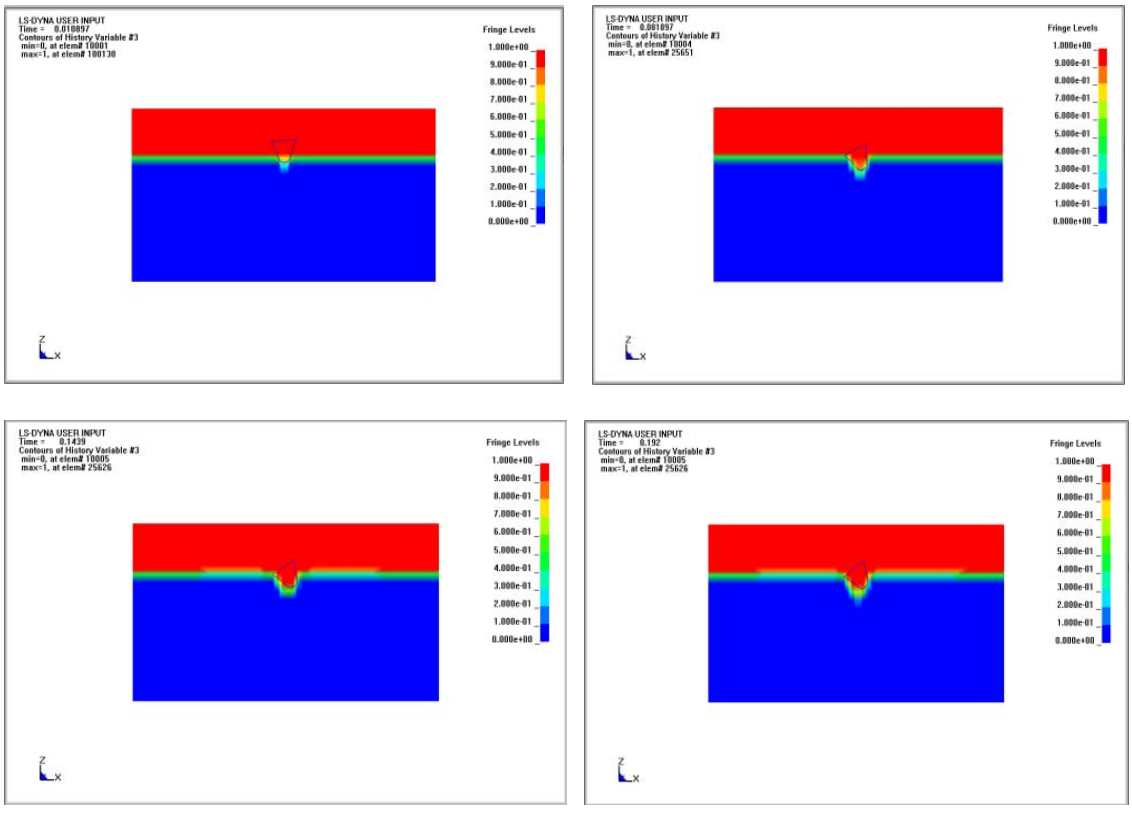

Fig. 6 Animation images at various time steps for 15 deg impact

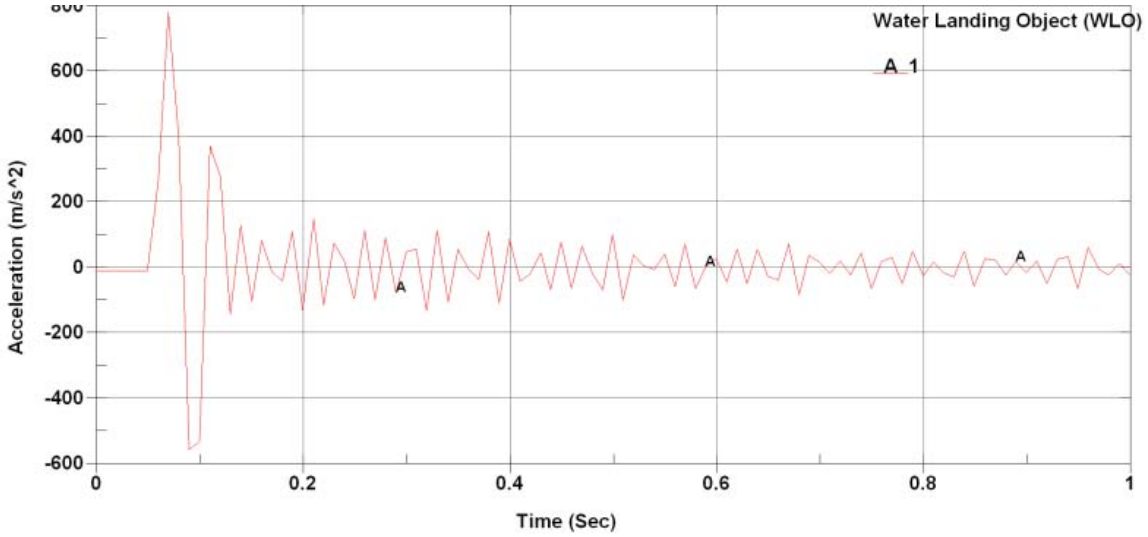

Fig. 7 Acceleration vs. Time for a 15 deg impact (V=9.8m/s)

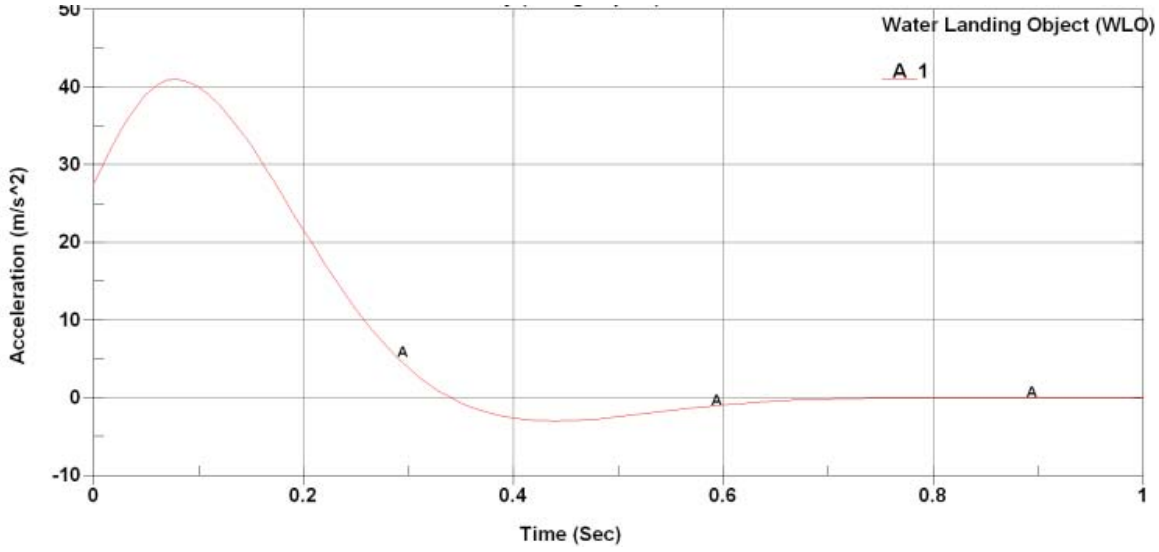

Fig. 8 Acceleration vs. Time for a 15 deg impact (9.8 m/s)
[Filtered acceleration time series (Sawtooth filter @1400Hz)]

Table 2: Summary of the pitch tests (V=9.8m/s)

Entry Angle (Deg)	Maximum Acceleration (m/s^2)
0	51.52
15	41.08
30	25.01
45	10.78

Effects of Weight Variation -- The effects of variations in the object weight were examined by varying object weights ranging from 2.5 kg to 5 kg (3.5kg corresponds to the experimental case-II involving an electromagnetic drop mechanism). Results for four different cases of model weights analyzed are shown in Table 3. The general trend shows a small advantage gained in reduced the g-force for a large increase in weight. Trends obtained from acceleration time history data for a 3.5 kg model was similar to the one attained for case-I. The acceleration time history for a weight of 3.5kg of WLO yields a value of 35.48 m/s^2. Table 4 shows the comparison of experimental results from the electromagnetic release mechanism with the ALE formulation. The peak acceleration from the FE simulations and the experimental data for case –II are 35.50 m/s^2 and 36.50 m/s^2, respectively, showing good predictive capability of the numerical model.

Table 3: Summary of the Weight Tests (V=9.8m/s)

Weight (kg)	Maximum Acceleration (m/s^2)
2.03	51.52
2.5	45.20
3.5	35.48
5.0	26.24

Table 4: Results for maximum acceleration filtered @ 1400 Hz [Weight of WLO = 3.5kg (Vertical Entry/Entry Angle=0 deg)]

Vertical Velocity at impact (m/s)	Maximum Acceleration (Numerical) (m/s^2)	Maximum Acceleration (Experimental) (m/s^2)	Percent Deviation (%)
9.81	35.50	36.50	2.74
9.3	31.15	31.72	1.96
8.8	26.98	27.32	1.24
8.1	22.39	22.82	1.76
7.5	19.32	19.55	1.17
7.0	14.92	15.32	2.25
6.2	11.90	12.12	1.81
5.3	10.4	10.72	2.98
4.4	9.64	9.92	2.86

4 Analytical description of the general impact-contact problem

Bounds on maximum acceleration due to impact of a rigid object water re-entry can be obtained analytically (Scolan and Korobkin 2001). For a rigid object with a spherical bottom, closed form solutions based on the von Karman and Wagner approaches are available for correlating with the results from the explicit finite element analyses (Wang and Lyle 2007). The boundary conditions for the analytical approach involve the free surface kinematic boundary condition, the free surface dynamic boundary condition and

the radiation boundary condition. The linearized dynamic condition also imposes that fluid particles of the free surface can move only vertically. The pressure on the body is determined according to Bernoulli equation, and the impact force on the body can be obtained by direct integration of the pressure over the wetted body surface theory.

The magnitude of the virtual mass for a spherical bottom body is

$$m_v = \frac{4}{3}\rho h^{\frac{3}{2}}(2R-h)^{\frac{3}{2}} \tag{5}$$

Where m_v is the virtual mass, ρ is the mass density of water, h is the water depth, and R is the radius of the spherical bottom.

Assuming $\frac{h}{R}$<<1, the maximum acceleration can be found as

$$a_{\max} = -\frac{256}{243}\left(\frac{4\pi\rho g R^3}{3W}\right)^{\frac{2}{3}}\left(\frac{V_0^{\,2}}{gR}\right) \tag{6}$$

Recently, Miloh used a semi-Wagner approach to determine the slamming coefficient, a non-dimensional parameter. Based on these analytical derivations, Miloh proposed that the maximum acceleration can be estimated as

$$a^*_{\max} = \frac{g}{2W}C_s\left(\frac{h_{\max}}{R}\right)\rho\pi R^2 V_0^{\,2} \tag{7}$$

Table 5 shows the comparison of the experimental results (setup-I and setup-II) with analytical solutions using von Karman and Wagner approaches. The maximum Z-acceleration for a vertical entry for both the drop mechanisms is bounded by the closed form solutions based on von Karman and Wagner approaches.

Table 5: Analytical solution results from von Karman and Wagner approaches

Water Landing Object (WLO) Experimental Cases	**Maximum acceleration g: acceleration due to gravity ($\frac{m}{s^2}$)**		**Analytical Solutions for maximum accelerations**		**Equivalent Radius (m) of WLO conical portion**	
Cone radius: 0.0848m Max. Radius: 0.3385m	**Experimental (Drop Tests)**	**Numerical (FE tests)**	**von Karman (Eq.5)** $a_{\max}$	**Wagner (Eq. 10)** $a^*_{\max}$	**von Karman** $r_{\max}$	**Wagner** $r^*_{\max}$
Case-I: Ordinary drop mechanism	5.2g	5.1g	14.7g	19.8g	0.0300 m	0.1075 m
Case-II: Electromagnetic release mechanism	3.6g	3.5g	10.4g	25.2g	0.0293 m	0.1310 m

It is important to note that the maximum radius of the base (for a 1/6th Froude-scale model of WLO) is 338.5mm and the radius of the conical portion impacting the water surface is 84.8mm. For a conical bottomed rigid object, the analytical results show that there is large difference between the experimental peak impact accelerations and those obtained by von Karman and Wagner analytical estimates. The large difference can be attributed to the conical shape of WLO bottom impacting the water surface compared to the large spherical bottom used in deriving the closed form solutions. In addition to the unique shape of the WLO the basic assumptions of the formulations for both von Karman and Wagner approaches also play a pivotal role in contributing to the large difference. The von Karman approach is based on the momentum theorem (using an added virtual mass) and the penetration depth is determined without considering the splash-up of the water level, thus neglecting the highly nonlinear coupled fluid-structure interaction effect. The Wagner approach, on the other hand, attempts to relax the von

Karman no-splashing assumption by using a rigorous dynamic formulation and incorporates the effect of the upward splashing of the water and its effects on the object. With the upward splashing correction, the Wagner approach tends to over predict the maximum impact retardation as it neglects the water compressibility (i.e. a more yielding fluid) near the impact zone.

5 Smoothed Particle Hydrodynamics (SPH) Simulations

Smoothed particle hydrodynamics (SPH) is an N-body integration scheme developed by Lucy Gingold and Monaghan (1977) to avoid the limitations of mesh tangling encountered in extreme deformation problems with the FE method. The main difference between classical methods and SPH is the absence of grid. Hence, the particles are the computational framework on which the governing equations are resolved. The main advantage, however, arises directly from its Lagrangian nature, since such an approach can tackle difficulties related with lack of symmetry, large voids that may develop in the field, and a free water surface much more efficiently than Eulerian methods can. The conservation laws of continuum fluid dynamics, in the form of partial differential equations, are transformed into particle form by integral equations through the use of an interpolation function that gives kernel estimation of the field variables at a point (Hallquist 1998). The Gruneisen equation of state that was used for the ALE method was retained for simulation the water domain that was modeled using a Null material model. However, the speed of sound at the reference density was set to 100m/s as the acoustic

speed is not important for the present problem. It is worthy to note that this sound speed is much lower than that of a real fluid, but much faster than any water waves in the model.

SPH Formulation--- The particle approximation function is given by:

$$\prod^h f(x) = \int f(y) W(x-y,h)dy \tag{8}$$

where W is the kernel function. The Kernel function W is defined using the function θ by the relation:

$$W(x,h) = \frac{1}{h(x)^d}\theta(x) \tag{9}$$

where d is the number of space dimensions and h is the so-called smoothing length which varied in time and space. $W(x,h)$ is a centrally peaked function. The most common smoothing kernel used by the SPH is the cubic B-spline which is defined by choosing θ as:

$$\theta(u) = Cx\begin{cases} 1-\frac{3}{2}u^2+\frac{3}{4}u^3 & \text{for } |u| \le 1 \\ \frac{1}{4}(2-u)^3 & \text{for } 1 \le |u| \le 2 \\ 0 & \text{for } 2 < |u| \end{cases} \tag{10}$$

where C is a constant of normalization that depends on the spatial dimensions.

The particle approximation of a function is now defined by:

$$\prod^h f(x_i) = \sum_{j=1}^{N} w_j f(x_i) W(x_i - x_j, h) \tag{11}$$

where $w_j = \frac{m_j}{\rho_j}$ is the "weight" of the particle. The weight of a particle varies proportionally to the divergence of the flow.

Discrete form of conservation equation--- The conservation equations are written in their discrete form and the momentum conservation equation is:

$$\frac{dv^{\alpha}}{dt}(x_i(t)) = \frac{1}{\rho_i}\frac{\partial(\sigma^{\alpha\beta})}{\partial x_i}(x_i(t)) \tag{12}$$

where α, β are the space indices.

Energy conservation equation is given by:

$$\frac{dE}{dt} = -\frac{P}{\rho}\nabla v \tag{13}$$

Artificial Viscosity---The artificial viscosity is introduced when a shock is present. Shocks introduce discontinuities in functions. The role of artificial viscosity is to smooth the shock over several particles. To take into account the artificial viscosity, an artificial viscous pressure term Π_{ij} [Monaghan and Gingold 1983] is added such that:

$$p_{i\rightarrow} p_{i+}\Pi_{ij} \tag{14}$$

Where $\Pi_{ij} = \frac{1}{\bar{\rho}_{ij}}(-\alpha\mu_{ij}\bar{c}_{ij} + \beta\mu_{ij}^2)$. The notation $X_{ij} = \frac{1}{2}(\bar{X}_i + X_j)$ is used for median between X_i and X_j, c is the adiabatic sound speed, and

$$\mu_{ij} = \begin{cases} \bar{h}_{ij} \dfrac{v_{ij} r_{ij}}{r_{ij}^2 + \eta^2} & \text{if} \quad v_{ij} r_{ij} < 0 \\ \\ 0 & \textit{otherwise} \end{cases} \tag{15}$$

Here, $v_{ij} = (v_i - v_j)$, and $\eta^2 = 0.01 \bar{h}_{ij}^2$ which prevents the denominator from vanishing.

Time Integration--- A simple and classical first-order scheme for integration is used. The time step is determined by the expression:

$$\delta t = C_{CFL} Min\left(\frac{h_i}{c_i + v_i} \right) \tag{16}$$

where the factor C_{CFL} is a numerical constant.

Description of the SPH model---Water was simulated by using SPH elements. A water body of 4m (diameter) x 2m (length), modeled as a cylindrical mesh, was chosen for the impact studies. The edges of the water were defined as fixed-SPH nodes allowing the water block to be relatively small in size. Figure 9 shows the plan of the water-space capsule SPH discrete particle mesh. The same material properties were retained for the rigid object and the water domain for the SPH simulations.

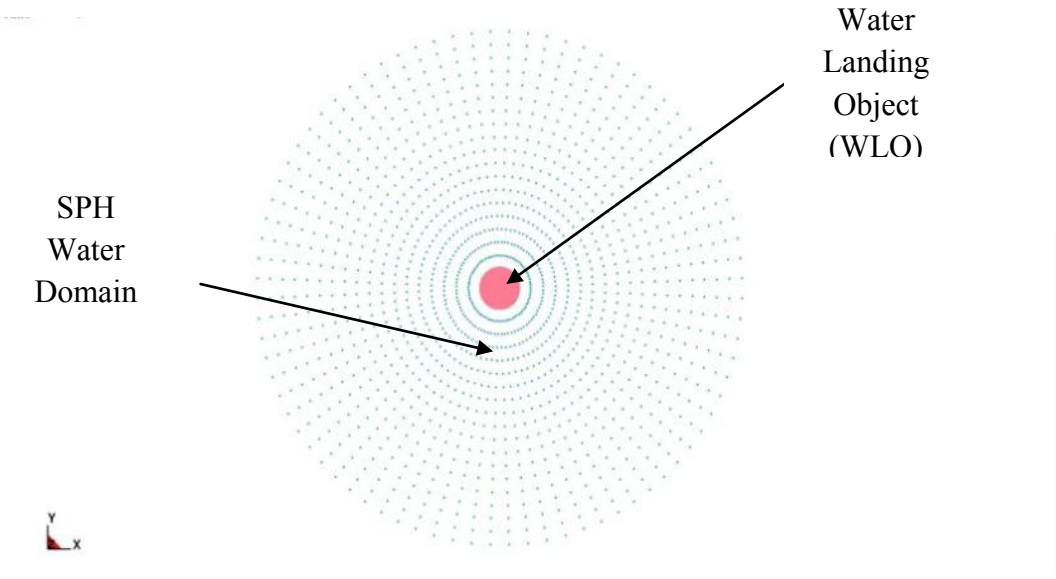

Fig. 9 Plan of the SPH Water domain and the WLO

Effects of Vertical Velocity Variation ---The vertical velocities ranged from 10m/s to 4 m/s, of which 9.81 m/s corresponds to the nominal scaled down impact velocity upon water landing. The elevation of the mesh impingement using the SPH formulation is shown in Figure 10. Filtered acceleration time history is shown in Figure 11 (peak impact acceleration is 51.05m/s^2).

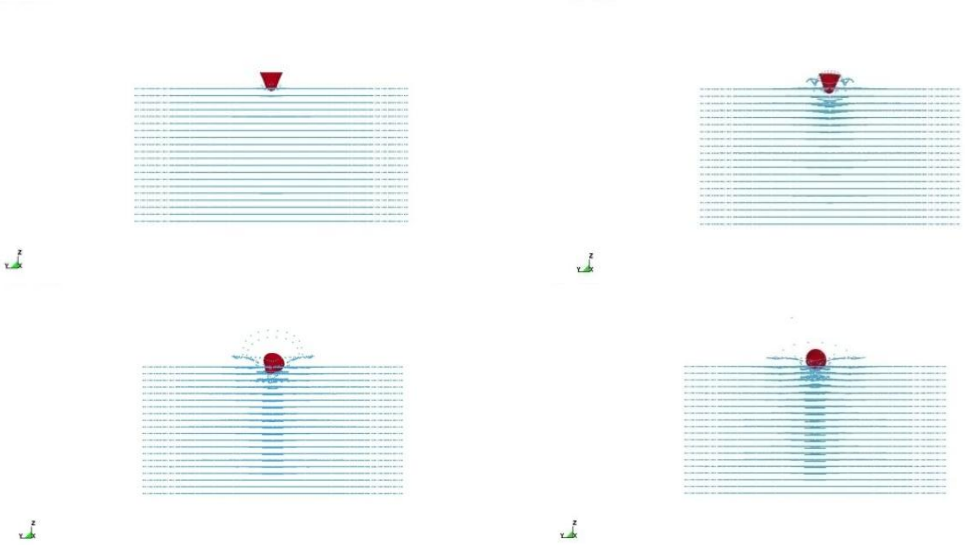

Fig. 10 Elevation view of the particle mesh impingement using the SPH method

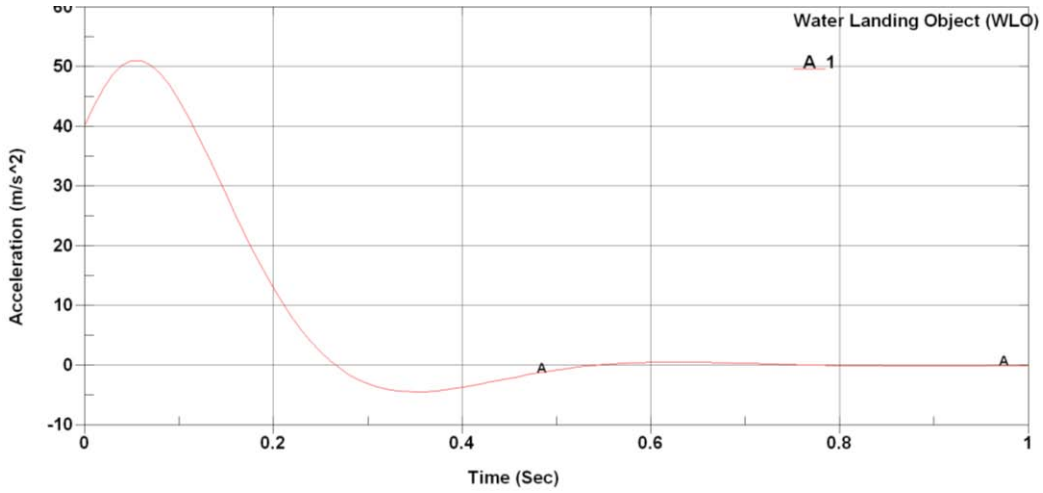

Fig. 11 Filtered Acceleration time history (Sawtooth filter @ 1156 Hz)

Figure 12 shows a good comparison between the experimental results and the ALE and SPH results for maximum impact acceleration. The graph indicate that the trend of impact accelerations increased and happening must faster with an increase in the entry speed. Figure 12 also shows the plot of accelerations obtained analytically vs. drop

height for the WLO model (using the original radius of the WLO). It is important to note the values of maximum impact accelerations are almost identical for both von Karman and Wagner solutions.

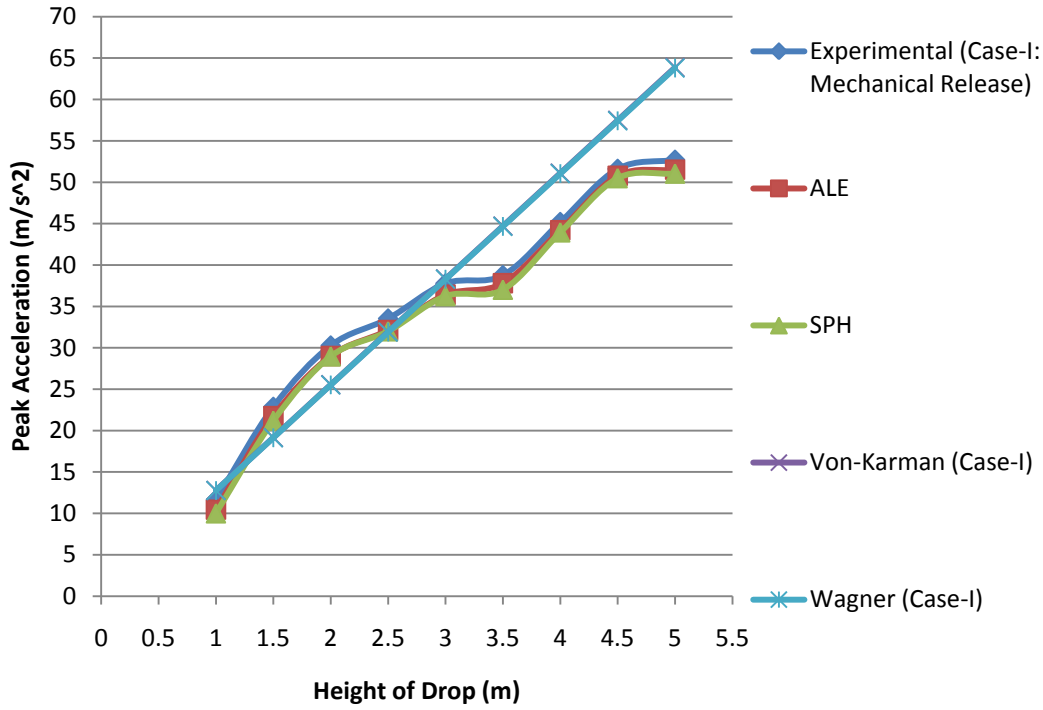

Fig. 12 Comparison of results for maximum acceleration with ALE and SPH [Weight of WLO = 2.03 kg (Case-I: Mechanical release)] (Vertical Entry/Entry Angle=0 deg)

Effects of Entry Angle Variation (Pitch Tests) --- To determine the effect of varying the entry angle of the WLO upon impact, the entry angle was varied from 15 to 30 deg. Comparative results with ALE from these tests are shown in Figure 13. As expected, the impact acceleration can be reduced by having the WLO enter the water at an angle. It is also important to note that the SPH results match reasonably well with the ALE results

for the inclined impact tests. Note that there are not experimental results to calibrate the numerical predictions (no angle variation tests were conducted). However, it is nevertheless interesting to observe the closeness of prediction results obtained by the two numerical models. This also demonstrates the usefulness of numerical simulations once the models have been calibrated by other experimental data.

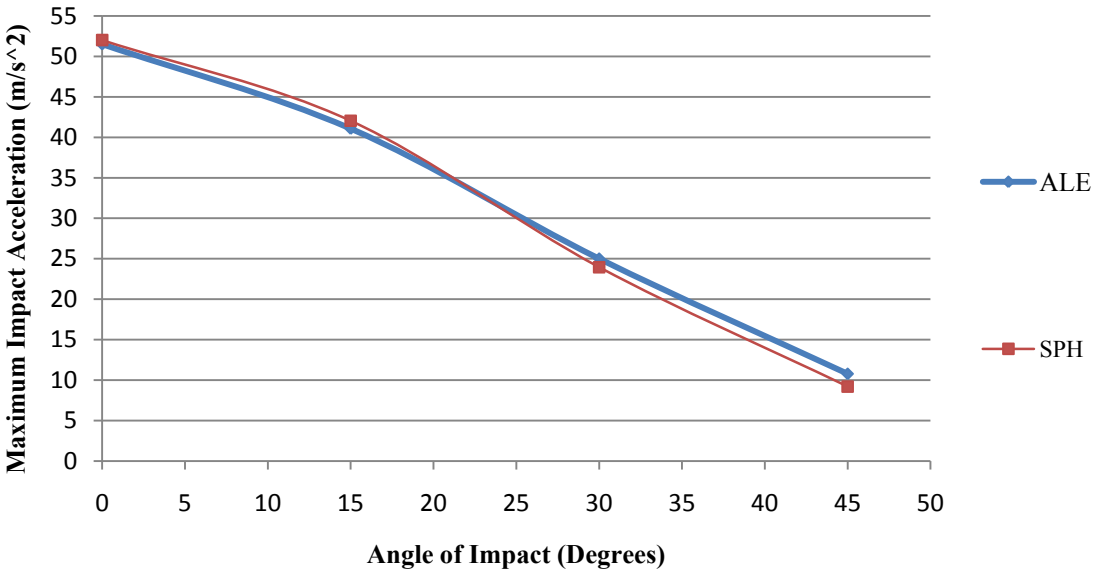

Fig. 13 Comparison of impact acceleration for pitch tests using ALE and SPH methods

Effects of Weight Variation --- The effect of varying the WLO weight was obtained by testing weights ranging from 2.5 kg to 5 kg. A test for 3.5 kg corresponds to the experimental case-II involving an electromagnetic drop mechanism. It can be seen from the results that as the object gets heavier the impact accelerations reduce dramatically. The general trend shows a small advantage gained in reduced *g*-force for a large increase in weight. The acceleration data obtained was filtered as in the ALE case and the filtered

acceleration time history for a weight of 3.5kg of WLO yields a value of 35.48 m/s^2. Figure 14 shows the comparison of experimental results from the electromagnetic release mechanism with the ALE and SPH formulation. Observe that the peak acceleration decreases linearly with the successive decrease in the height of drop and the peak acceleration is reduced due to the increase in the weight of WLO. Importantly, there is good comparison of the experimental results with both the numerical simulations.

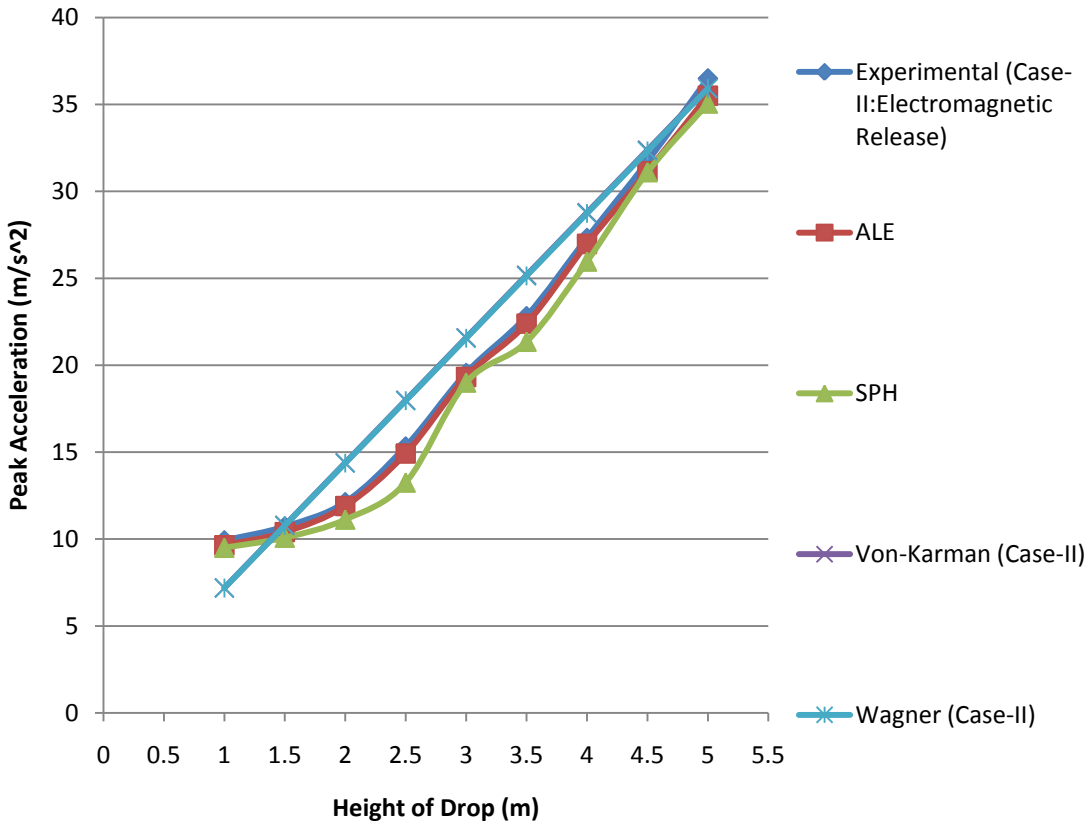

Fig. 14 Comparison of results for maximum acceleration with ALE and SPH [Weight of WLO = 3.5kg (Case-II: Electromagnetic release)] (Vertical Entry/Entry Angle=0 deg)

The plot of accelerations obtained analytically vs. drop height for the WLO model (using the original radius of the WLO) is shown in Figure 14. The plot also depicts that the values of maximum impact accelerations (obtained analytically) are almost similar for both von Karman and Wagner solutions.

6 Performance studies of ALE and SPH

Solving practical engineering analysis problems often requires use of large-scale numerical models (which can have several thousands or millions of nodes and elements) and access to the high-performance computing (HPC) platforms to achieve reasonable accuracy. Advanced numerical codes like ALE and SPH need such HPC platforms clubbed with a definitive model size to solve real time FSI problems. Model size plays a pivotal role in not only capturing the physics of the problem but also determines the computational effort needed to reach the full termination time.

In addition to the model size, the run times also plays a significant role in determining the choice of the numerical code. This inherently provides the end users and scientists to proceed with a balanced approach in making a choice in terms of the available hardware, optimum model size and the accuracy in obtaining satisfactory test results.

The performance of ALE and SPH model tests were studied for the typical case of a vertical impact of the WLO. The ALE test case had 12,567 nodes and 11,680 elements whereas the SPH case had 33,526 nodes. The model was run on the OSU HPC platform on various nodes and the estimated clock time was recorded for each run. Table 6 shows

the execution time taken to compile the jobs on a single cluster by varying the number of CPUs. It also reports the speedup scale factors [which is the ratio of clock time using a single processor divided by the clock time using multiple processors ($=N_1/N_p$)]. The ratio of execution time for both ALE and SPH are also shown in the performance table.

Figure 15 graphically illustrate the performance using even number of processors (for two difference numerical test cases). Figure 16 graphically demonstrates the ratios of the execution times for both ALE and SPH using number of CPUs. All these figures indicate that as the number of CPUs increases there is a significant reduction in the estimated clock time. The performance studies also reveal that the number of nodes used in the ALE tests is approximately three times the number of nodes used in the SPH tests, but the ALE formulation is about 12 times faster than the SPH method. As evident from these figures, the user is now equipped with interesting design choices with the number of processors to achieve an optimal clock time for a given model.

Ideally it is desirable to have linear speedup with respect to the number of processors used to run the model. However, Fig. 17 shows the (speedup) scaling performance of ALE and SPH with increasing number of nodes. Note that scaling performance is far below linear and that they both show a similar trend. Hence, there is little gain in using more than 8 processors for either of the numerical models.

Table 6 Performance study for the ALE and SPH test models

ALE test model: Number of time steps = 7436 SPH test model: Number of time steps = 15098					
Number of processors (ncpu)	**ALE execution time (seconds)**	**ALE-Speedup (N_1/N_p)**	**SPH execution time (seconds)**	**SPH-Speedup (N_1/N_p)**	**SPH/ALE clock-time ratios**
1	1860	1	23940	1	12.87
2	1386	1.34	17340	1.38	12.51
4	1279	1.45	15420	1.55	12.05
6	1148	1.62	13690	1.74	11.92
8	913	2.03	12239	1.95	13.40
10	876	2.12	11134	2.15	12.71

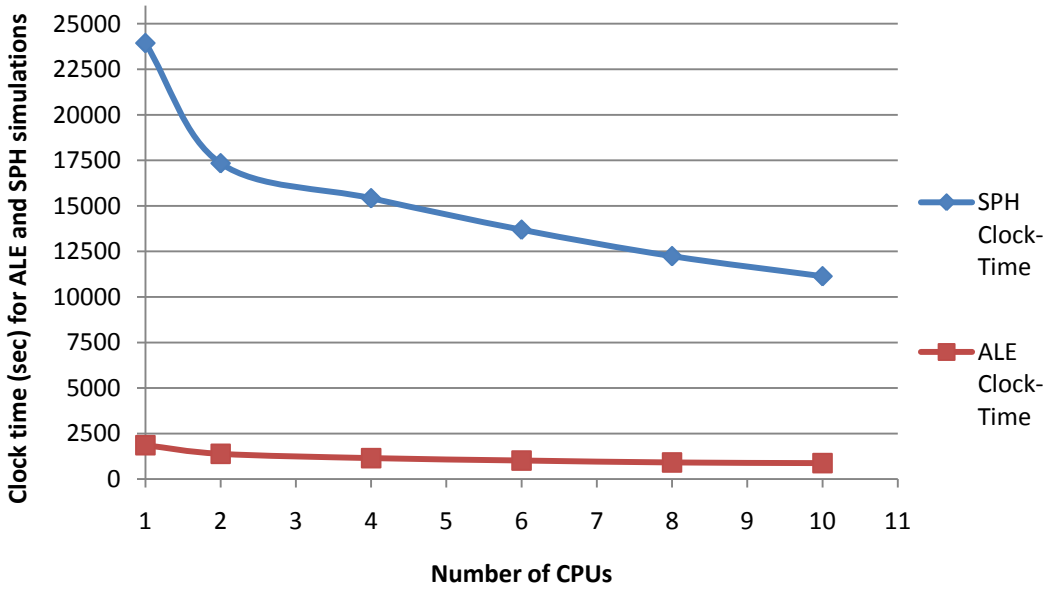

Fig. 15 Number of CPUs vs. estimated clock time for ALE and SPH test models (Total number of nodes: 33626/Total number of SPH nodes: 32000) (Total number of nodes: 12567/Total number of elements: 11680)

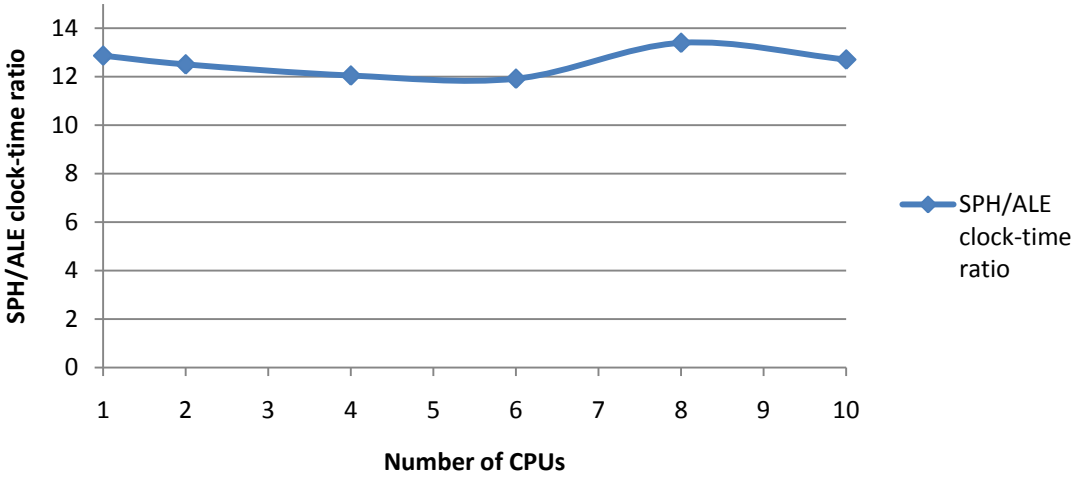

Fig. 16 Clock-time ratios of SPH/ALE vs the number of CPUs

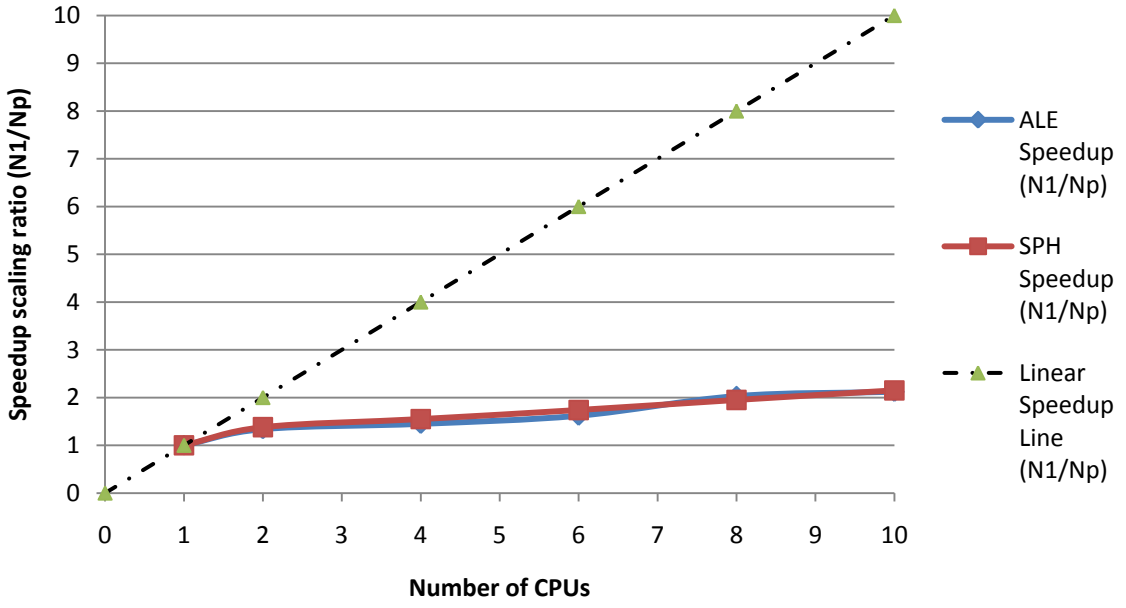

Fig. 17 Speed scaling of the performance of ALE and SPH (N_1/N_p)

7 Discussion and Comparison

The study of hydrodynamic impact between a body in motion and a water free-surface finds variety of applications in the aerospace and ocean engineering fields. The analytical approaches put forth by von Karman, Wagner and others provide us with the beginnings for a complete solution of the impact phenomena through use of numerical techniques such as finite elements. The effects of varying the vertical velocity, entry angle and the WLO weight were identified and the numerical results obtained from these tests help us understand and establish conditions that must be avoided during the water impact. For instance, if a crew member onboard the WLO cannot withstand impact accelerations over $5\,g$, these results will give a glimpse of the initial conditions which will keep the peak impact accelerations under the specified limits.

The application of multi-material Eulerian formulation and a penalty based Lagrangian-Eulerian coupling algorithm combined with a proper working model for fluids is shown to capture the water landing well. The current work, simulating the complex impact event, using ALE and SPH techniques, demonstrates some of the problems encountered when modeling water. The robust contact-impact algorithm of the current FE code simulated the behavior of water for a very short duration of time and the initial period was sufficiently long to establish the trends occurring under a wide range of conditions.

Fluid properties of water are defined by the bulk modulus that gives relation between the change of volume and pressure. Reducing the speed of sound in water in the input to the order of about 10 times the celerity of wave, causes a significant reduction in the bulk

modulus, thereby resulting in faster execution time as the time step becomes bigger. Because the focus of the wave impact behavior is gravity dominated and not sound propagation sensitive. This technique provides a faster solution without sacrificing accuracy.

The acceleration values obtained from the FE results compared well (after proper filtering techniques) with experimental values. Importantly, there is a good comparison between the experimental and the ALE and SPH results for maximum impact accelerations for all the three cases of varying the vertical velocity, entry angle and the weight of the object.

The application of multi material ALE technique and a penalty based coupling algorithm (used for large deformation of water at the free surface upon impact) currently can be properly analyzed only at the cost of high computational time. Use of the SPH method is notably less complicated in generating the model due to the absence of mesh and the ease with which it can successfully model the large deformation problems involving the water domain. The main advantage of using SPH is that it can capture the post impact dynamics (buoyancy effect) more graphically. However, the computational effort required of the SPH method is significantly higher than that of ALE.

An attempt was made to measure the pressure distribution and the structural deformation coming onto the WLO by treating it as a flexible body, to compare both ALE and SPH codes, but it was discarded due to the high computational time and expense.

The WLO was assumed as rigid for convenience of comparison of the numerical results with closed form solutions for maximum accelerations predicted by the classical von Karman and Wagner. In order to emphasize the importance of the analytical estimates, the accelerations obtained analytically were plotted against the drop height for the WLO model (using the original radius of the WLO). In order to achieve accelerations comparable to the closed-form solutions, the analytical results show that, for the design of a WLO, the Wagner approach provides a reasonably correct estimate of the equivalent radius of the WLO.

8 Concluding Remarks

A preliminary study of simulating the water landing of a conceptual Water Landing Object with an explicit numerical code is presented. The non-linear transient dynamic code with its finite-element ALE and SPH capability for analyzing large deformation structural and fluid dynamic applications is used to model the scaled down experiments. The present work is the first of its kind in testing a scaled-down model of WLO impacting ocean waters for the Indian Space Mission. An important aspect in evaluating the predictive capability of the FE-ALE and SPH is the accuracy and reliability of the numerical simulation results in determining the impact accelerations.

The water domain is modeled using an equation of state with a reduced speed of sound. A constrained Lagrange interface/contact is shown to successfully capture impact phenomenon between the object and the water target.

The effects of varying the vertical velocity, entry angle and the WLO weight are identified and the numerical predictions are first validated with experimental data for maximum impact accelerations. The maximum acceleration upon impact is about 5.1g for a 0-degree pitch angle (vertical velocity tests) and 4.1g for a 15-degree pitch test (pitch tests). Analyses were performed for the rigid object entering the water with different weights. The weight of 3.5kg corresponds to the experimental Case-II involving an electromagnetic drop mechanism. The general trend shows advantage gained in reduced g-force for a large increase in weight (3.5g for Case-II compared to 5.1g for Case-I). This indicates that the analyses performed can produce satisfactory results to use in design studies.

A numerical analysis was performed on the WLO prototype using FE-ALE and SPH methods to predict the peak acceleration value at touchdown for an impact velocity of 60 m/s. The predicted acceleration time histories gave a peak acceleration value of 5.3g, which is in good agreement with the FE simulations performed on the scaled-down model of WLO (5.2g).

Tasks performed in this study also include the comparison of the numerical solutions with analytical solutions for the rigid object and understanding the filtering techniques needed to predict the correct maximum impact accelerations. These predictions suggest that the fully coupled FSI models can capture the water-impact response accurately for all range of drop tests and there is a good comparison between the simulations and the experimental results.

Several observations can be made. Model testing is needed over a wider range of conditions to include improved tests that vary the speed, weight and entry angle and under realistic conditions existing in the oceans. Modeling of the rigid body impact problem used for correlation with the experimental results, demonstrates some of the challenging problems encountered when modeling the water domain. There is a need for a better solver, with a robust characterization of water, to run the FE models for longer durations to fully capture the buoyancy effect on the WLO motion.

The possibility of combining the finite element package with a computational fluid dynamics package could more accurately simulate the hydrodynamics during impact. Filtering techniques need to be understood better in order to make better engineering judgments from the computed data. Further levels of complexity can be introduced to the model as well as scrutinizing the results further. Future work may include more in-depth analysis of the WLO water impact pressures, fully deformable vehicles and floatation studies. The development of a more accurate numerical solution to capture the nonlinear nature of the FSI problem should be pursued by employing robust modeling of the basic physics of water impact. Finally, full-scale prototype testing is needed over a wider range of conditions to include cases with varying speed, weight and entry angle under realistic conditions existing in the oceans.

Acknowledgements

The authors gratefully acknowledge the valuable comments and suggestions by the conference papers reviewers and discussions with experts in the area especially Professor Odd Faltinsen. Financial support from the US Office of Naval Research Grants N00014-10-10230 and N00014-11-10094, and the National Science Foundation Grants CMS-0217744 and CMS-0530759 for the first and second authors is gratefully acknowledged.

References

Belytschko, T., Flanagran, D. F., and Kennedy, J. M., 1982. "Finite element method with user-controlled meshes for fluid-structure interactions," *Comput. Methods Appl. Mech. Eng.,* **33**, pp. 689–723.

Benson, D., 1989. "An efficient accurate, simple ALE method for non linear finite element programs," *Comput. Methods Appl. Mech. Eng*., **33**, pp. 689–723.

Donea, J., Ponthot, J.P., Rodríguez F. A., and Huerta, A., 2004. "Arbitrary Lagrangian-Eulerian methods," *Encyclopedia of Computational Mechanics*, **3**, Wiley publications.

Faltisen, O. M., 1990. "Sea loads on ships and offshore structures," Cambridge University Press, Cambridge.

Faltinsen, O. M., and Zhao, R., 1997. "Water entry of ship sections and axisymmetric bodies," *AGARD FDP Workshop on High Speed Body Motion in Water held in Kiev, Ukraine, 1-3 September.*

Hallquist, J. O., 1998. "LS-DYNA Theoretical Manual," *Livermore Software Technology Corporation.*

Hirano, Y., and Miura, K., 1970. "Water impact accelerations of axially symmetric bodies," *Journal of Spacecraft Rockets*, **7**(6), pp. 762-764.

Jackson, K. E., and Fuchs, Y. T., 2008. "Comparison of ALE and SPH simulations of vertical drop tests of a composite fuselage section into water," *10th International LS-DYNA Users Conference*, June 8-10, Dearborn, Michigan, USA

Korobkin, A. A., 2004. "Analytical models of water impact," *European Journal of Applied Mathematics*, **15**, pp. 821-838.

Korobkin, A. A., and Scolan, Y. M., 2006. "Three-dimensional theory of water impact. Part 2. Linearized Wagner problem," *Journal of Fluid Mechanics*, **549**, pp. 343-373.

Laursen, T.A., 2002. "Computational Contact and Impact Mechanics – Fundamentals of Modeling Interfacial Phenomena in Nonlinear Finite Element Analysis," First Edition, Springer

Lin, Y. Y., 2002. "Performance evaluation on the ALE formulation in MPP," *7th International LS-DYNA Users Conference,* May 19-21, Dearborn, Michigan, USA.

Miloh, T., 1991. "On the initial-stage slamming of a rigid sphere in a vertical water entry," *Applied Ocean Research*, **13**(1), pp. 43-48.

Scolan, Y. M., and Korobkin, A. A., 2001. "Three-dimensional theory of water impact. Part 1. Inverse Wagner problem," *Journal of Fluid Mechanics*, **440**, pp. 293-326.

Seddon, C. M., and Moatamedi, M., 2006. "Review of water entry with applications to

aerospace structures," *International Journal of Impact Engineering*, **32**, pp. 1045-1067.

Souli, M., Olovsson, L., and Do, I. 2002. "ALE and fluid-structure interaction capabilities in LS-DYNA," *7th International Users Conference,* May 19-21, Dearborn, Michigan, USA.

Wagner, H., 1932. "Trans. Phenomena associated with impacts and sliding on liquid surfaces," *Math Mech,* **12**(4), pp. 193-215.

Wang, J. T., and Lyle, K. H., 2007. "Simulating space capsule water landing with explicit finite element method," 48th AIAA/ASME Conference,April, pp. 23-26, Waikiki, HI, USA.

Wriggers, P., 2002. "Computational Contact Mechanics," John Wiley & Sons Ltd.

Wriggers, P., and Nackenhorst, U., 2005. "Analysis and Simulation of Contact Problems," Springer

Wriggers, P., 2006. "Computational Contact Mechanics," II Edition, Springer Link

Zhao, R., and Faltinsen, O., 1993. "Water entry of two-dimensional bodies," Journal of Fluid Mechanics, **246**, pp. 593-612.

Chapter-4

Concluding Remarks and Future Research

Determining the hydrodynamic forces on a structure or the motion of objects resting on the ocean bottom (coupled wave-structure-seabed interaction) forms an intrinsic component of any typical FSI problem. This dissertation is aimed at evaluating the predictive capability of an advanced multi-numerical solution techniques approach to critically evaluate the contact and impact dynamic modeling capabilities of a finite element code LS-DYNA for coupled FSI problems.

An important aspect in the assessment of recovery and escape systems is the performance of such objects in ocean water landing. A distinguishable facet of this study is the comparison of the shape of space capsule used for the Indian and American space missions. The WLO used for the Indian space mission is conical in shape with a rounded nose than compared to the convex shape of the base used for all the American space missions. This significantly inhibits the comparison with the literature available for ACM or other American space missions. The present work is the first of its kind in testing a scaled-down model of WLO (with a conical shaped base) impacting ocean waters. However, the results obtained from the WLO experiments can be used to qualitatively justify the impact accelerations and touchdown pressures coming on to the object.

The primary objective is to study the dynamics of a WLO during water impact by performing experiments using a $1/6^{th}$ Froude-scale model of a using two independent

drop mechanisms. Drop Test I involved dropping the object using a rope and pulley arrangement, while Drop Test II employed an electromagnetic release to drop the object. The effects of varying the vertical velocity and the WLO weight are identified and the trend obtained helps the readers to comprehend the conditions that must be avoided during a water impact.

The hydrodynamic parameters such as peak acceleration, touchdown pressure and maximum impact force were measured and the dynamics during the touchdown of WLO was observed. For the WLO weighing 2.03kg (Drop Test I), the acceleration time series for a 10m/s velocity of impact gives a peak acceleration of 52.17 m/s^2 (~5.2g) and a touchdown pressure of 0.25bar and for the WLO tests with the electromagnetic release with an increased mass of 3.5kg of the model (Drop Test II), the peak acceleration was found to be 36.5 m/s^2 (~3.6g) and the touchdown pressure was computed as 0.49bar.

In addition, for both independent experimental data sets, the peak force was proportional to the square of the impact velocity, which is in good agreement with Kaplan‟s theoretical results. Hence, a formal comparison between the two cases cannot qualitatively demonstrate the efficiency of one case over the other. Instead, for an end user, an increased weight of WLO provides a measure of the reduction of the accelerations (3.6g in Drop Test II compared to 5.2g in Drop Test I). If a crew member onboard the WLO cannot withstand impact accelerations over 5g, these results will give a glimpse of the initial conditions which will keep the peak impact accelerations under the specified limits.

An important aspect is the accuracy and reliability of the experimental results in predicting the impact accelerations and touchdown pressures obtained from both the experimental cases. Results from both the experimental data sets show that the impact acceleration and touchdown pressure increases practically linearly with the increase in the height of the drop.

The peak impact force experienced by the model obtained using the model mass and measured acceleration is 105.9 N for Drop Test I compared to 127.725 N for Drop Test II. Comparison of drop heights to theoretical and experimental velocities depict a very good agreement for both the cases, ascertaining the accuracy of the impact accelerations measured experimentally for successive drop heights.

In order to describe the physics of the slamming problem, the maximum pressure obtained was compared to the pressure calculation when a circular cylinder slams water surface (Faltinsen 1990). The maximum pressure for both cases was well below the pressure bound ($\rho c_e V$). Interestingly, the horizontal component of velocity was found to have a very little effect on the accelerations in the vertical (Z) direction in both drop tests. No effort was made to measure neither the horizontal component of velocity nor the entry angle was varied.

The WLO was assumed as rigid for the convenience of comparing experimental results with closed form solutions for maximum accelerations predicted by the classical von Karman and Wagner. For a conical bottomed rigid object, the analytical results show that there is a large difference between the experimental peak impact accelerations and those obtained by these analytical estimates. The large difference can be partly attributed to the unique shape of the WLO and partly due to the assumptions of the formulations for both

von Karman and Wagner approaches. The maximum radius of the base of the model is 338.5mm whereas the radius of the conical portion impacting the water surface is 84.8mm which is primarily responsible for the large difference between experimental and analytical estimates. An improved approximate solution procedure using an "equivalent" radius concept integrating experimental results with the von Karman and Wagner closed-form solutions is proposed and developed in detail.

It can be observed that the von Karman approach tends to estimate a lower value of the radius of the conical portion whereas the Wagner approach tends to estimate a higher value of the impact radius. As the effect of local rise up of the water is significant during water entry of a rigid 3D object, the von Karman predictions for maximum impact accelerations are not significant in determining the maximum impact accelerations for the water entry of WLO. Based on the equivalent radius approach, the approximate analytical solutions of von Karman and Wagner can be used to obtain design maximum accelerations of the WLO model consistent with experimental results. Further, the mean equivalent radius (r*) was computed to analytically estimate the maximum impact accelerations (for varying impact velocities). Results show the maximum impact accelerations obtained by both the semi-analytical estimates compared reasonable well with the experimental acceleration values.

In order to achieve accelerations comparable to the closed-form solutions, the analytical results show that, for the design of a WLO, the Wagner approach provides a correct estimate of the equivalent radius of the WLO. It is, however, interesting to note that the acceleration values obtained by von Karman and Wagner solutions produce accelerations

that are similar ascertaining the importance of the shape of the WLO during water impact.

The analytical approaches put forth by von Karman, Wagner and others provide us with the beginnings for a complete solution of the impact phenomena through use of numerical techniques such as finite elements. A preliminary study of simulating the water landing of a conceptual Water Landing Object with an explicit numerical code was also presented. The non-linear transient dynamic code with its finite-element ALE and SPH capability for analyzing large deformation structural and fluid dynamic applications is used to model the scaled down experiments. An important aspect in evaluating the predictive capability of the FE-ALE and SPH is the accuracy and reliability of the numerical simulation results in determining the impact accelerations.

The application of multi-material Eulerian formulation and a penalty based Lagrangian-Eulerian coupling algorithm combined with a proper working model for fluids is shown to capture the water landing well. The water domain is modeled using an equation of state with a reduced speed of sound. A constrained Lagrange interface/contact is shown to successfully capture impact phenomenon between the object and the water target.

The current work, simulating the complex impact event demonstrates some of the problems encountered when modeling water. Fluid properties of water are defined by the bulk modulus that gives relation between the change of volume and pressure. Reducing the speed of sound in water in the input to the order of about 10 times the celerity of wave, causes a significant reduction in the bulk modulus, thereby resulting in faster execution time as the time step becomes bigger. Because the focus of the wave impact behavior is gravity dominated and not sound propagation sensitive. This technique

provides a faster solution without sacrificing accuracy. The robust contact-impact algorithm of the current FE code simulated the behavior of water for a very short duration of time and the initial period was sufficiently long to establish the trends occurring under a wide range of conditions.

The effects of varying the vertical velocity, entry angle and the WLO weight are identified and the numerical predictions are first validated with experimental data for maximum impact accelerations. The maximum acceleration upon impact is about 5.1g for a 0-degree pitch angle (vertical velocity tests) and 4.1g for a 15-degree pitch test (pitch tests). Analyses were performed for the rigid object entering the water with different weights. The weight of 3.5kg corresponds to the experimental Case-II involving an electromagnetic drop mechanism. The general trend shows advantage gained in reduced g-force for a large increase in weight (3.5g for Case-II compared to 5.1g for Case-I). This indicates that the analyses performed can produce satisfactory results to use in design studies.

The acceleration values obtained from the FE results compared well (after proper filtering techniques) with experimental values. Importantly, there is a good comparison between the experimental and the ALE and SPH results for maximum impact accelerations for all the three cases of varying the vertical velocity, entry angle and the weight of the object.

An attempt was made to measure the pressure distribution and the structural deformation coming onto the WLO by treating it as a flexible body, to compare both ALE and SPH codes, but it was discarded due to the high computational time and expense.

The application of multi material ALE technique and a penalty based coupling algorithm (used for large deformation of water at the free surface upon impact) currently can be

properly analyzed only at the cost of high computational time. Use of the SPH method is notably less complicated in generating the model due to the absence of mesh and the ease with which it can successfully model the large deformation problems involving the water domain. The main advantage of using SPH is that it can capture the post impact dynamics (buoyancy effect) more graphically. However, the computational effort required of the SPH method is significantly higher than that of ALE.

A numerical analysis was performed on the WLO prototype using FE-ALE and SPH methods to predict the peak acceleration value at touchdown for an impact velocity of 60 m/s. The predicted acceleration time histories gave a peak acceleration value of 5.3*g*, which is in good agreement with the FE simulations performed on the scaled-down model of WLO (5.2*g*).

Future Research

The advanced, state-of-the-art FE code LS-DYNA adopted in this project, when fully developed, will enhance the modeling, prediction, operation and control capabilities of the complex Fluid-Structure interaction in general and the numerical simulations of water entry problems in particular. The 3-D numerical codes being developed will provide additional tools to calibrate and validate the accuracy of the numerical predictions of the modules with laboratory experiment and field data. The fluid domain followed by the structure can be modeled using four different computational methods. The fluid domain will be modeled using the fully nonlinear potential flow (FNPF) or the boundary-element method (BEM). Reynolds averaged Navier-Stokes (RANS) and the particle finite element method (PFEM) will be used in the water/structure domain. The resulting numerical

predictive capability will be incorporated into an overarching computational framework for the analysis and simulation of the dynamic behavior of naval systems in the marine environment of arbitrary water depth.

Model testing is needed over a wider range of conditions to include improved tests that vary the speed, weight and entry angle and under realistic conditions existing in the oceans. Modeling of the rigid body impact problem used for correlation with the experimental results, demonstrates some of the challenging problems encountered when modeling the water domain. There is a need for a better solver, with a robust characterization of water, to run the FE models for longer durations to fully capture the buoyancy effect on the WLO motion.

The possibility of combining the finite element package with a computational fluid dynamics package could more accurately simulate the hydrodynamics during impact. Filtering techniques need to be understood better in order to make better engineering judgments from the computed data. Further levels of complexity can be introduced to the model as well as scrutinizing the results further. Future work may include more in-depth analysis of the WLO water impact pressures, fully deformable vehicles and floatation studies. The development of a more accurate numerical solution to capture the nonlinear nature of the FSI problem should be pursued by employing robust modeling of the basic physics of water impact. Finally, full-scale prototype testing is needed over a wider range of conditions to include cases with varying speed, weight and entry angle under realistic conditions existing in the oceans.

Bibliography

Baker, E., and Westine, S., 1967. "Model tests for structural response of Apollo Command Module to water impact," *Journal of Spacecraft and Rockets*, **4**(2), pp. 201-208.

Batchelor, G.K., 1967. "An Introduction to Fluid Dynamics," *Cambridge University Press,* Cambridge.

Belytschko, T., Flanagran, D. F., and Kennedy, J. M., 1982. "Finite element method with user-controlled meshes for fluid-structure interactions," *Computer Methods in Applied Mechanics and Engineering,* **33**, pp. 689–723.

Benson, D., 1989. "An efficient accurate, simple ALE method for non linear finite element programs," *Computer Methods in Applied Mechanics and Engineering*, **33**, pp. 689–723.

Brebbia, C.A., and Nurick, G.N., 2003. "Advanced in Dynamics and Impact Mechanics," WIT Press.

Challa, R., Idichandy, V.G., Vendhan, C. P., and Solomon, S. C. Y., 2010, "An Experimental study on rigid-object water-entry impact and contact dynamics," Proceedings of the 29th Internatio*nal Conference on Ocean, Offshore and Arctic Engineering (OMAE),* June 6-11, Shanghai, China.

Challa, R., Solomon, S. C. Y., Idichandy, V. G., and Vendhan, C. P., 2010, "Finite-Element and Smoothed Particle Hydrodynamics Modeling of Rigid-Object Water-Entry Impact and Contact Dynamics and Validation with Experimental Results," Proceedings of the 29th *International Conference on Ocean, Offshore and Arctic*

Engineering (OMAE), June 6-11, Shanghai, China.

Crespo, A.J.C., Gomez, G.M., Dalrymple, R.A., 2008. "Modeling Dam Break Behavior over a wet bed by a SPH technique," *Journal of Waterway, Port, Coastal, and Ocean Engineering*, **134**(6), pp. 313-320.

Faltisen, O. M., 1990. "Sea loads on ships and offshore structures," *Cambridge University Press,* Cambridge.

Faltinsen, O. M., and Zhao, R., 1997. "Water entry of ship sections and axisymmetric bodies," *AGARD FDP Workshop on High Speed Body Motion in Water,* Kiev, Ukraine.

Gingold, R.A., and Monaghan, J.J., 1977. "Smoothed particle hydrodynamics: Theory and application to nonspherical stars," *Monthly Notices of the Royal Astronomical Society*, **181**, pp. 375–389.

Gomez, M.G., and Dalrymple, R.A., 2004. "Using a three-dimensional smoothed particle hydrodynamics method for wave impact on a tall structure," *Journal of waterway, port, coastal and ocean engineering*, **130**(2), pp. 63-69.

Hallquist, J. O., 1998. "LS-DYNA Theoretical Manual," *Livermore Software Technology Corporation.*

Hirano, Y., and Miura, K., 1970. "Water impact accelerations of axially symmetric bodies," *Journal of Spacecraft Rockets*, **7**(6), pp. 762-764.

Kaplan, A., 1968. "Simplified dynamic analysis of Apollo water impact, including effects of the flexible heat shield," *11176-11176-6004-R0-00*, TRW, Redondo Beach, California, USA.

Korobkin, A.A., 2004. "Analytical models of water impact," *European Journal of*

Applied Mathematics, **15**, pp. 821-838.

Korobkin, A.A., and Scolan, Y.M., 2006. "Three-dimensional theory of water impact. Part 2: Linearized Wagner problem," *Journal of Fluid Mechanics*, **549**, pp. 343-373.

Laursen, T.A., 2002. "Computational Contact and Impact Mechanics – Fundamentals of Modeling Interfacial Phenomena in Nonlinear Finite Element Analysis," First Edition, Springer

Lin, Y. Y., 2002. "Performance evaluation on the ALE formulation in MPP," *7th International LS-DYNA Users Conference,* May 19-21, Dearborn, Michigan, USA.

Liu, G.R., and Liu, M.B., 2003. "Smoothed Particle Hydrodynamics: a meshfree particle method," *World Scientific*, Singapore

Miloh, T., 1991. "On the initial-stage slamming of a rigid sphere in a vertical water entry," *Applied Ocean Research*, **13**(1), pp. 43-48.

Monaghan, J.J., 1994. "Simulating free surface flows with SPH," Journal of Computational Physics, **110**, pp. 399–406.

Owen, D.R.J., and Hinton, E., 1980. "Finite Elements in plasticity: Theory and practice," *Pineridge Press*, Swansea, U.K.

Scolan, Y. M., and Korobkin, A.A., 2001. "Three-dimensional theory of water impact. Part 1. Inverse Wagner problem," *Journal of Fluid Mechanics*, **440**, pp. 293-326.

Seddon, C. M., and Moatamedi, M., 2006. "Review of water entry with applications to aerospace structures," *International Journal of Impact Engineering*, **32**, pp. 1045-1067.

Smith, H.D., 2004. "Modeling the flow and scour around an immovable cylinder," *MS*

Thesis, *Department of Civil and Environmental Engineering and Geodetic Science*, Ohio State University, USA.

Souli, M., Olovsson, L., and Do, I., 2002. "ALE and fluid-structure interaction capabilities in LS-DYNA," *7th International Users Conference,* May 19-21, Dearborn, Michigan, USA.

Tokura, S., and Tetsuli, I., 2005. "Simulation of wave dissipation mechanism on submerged structure using fluid-structure coupling capability in LS-DYNA", *5th European LS-DYNA users conference*, pp. 2c-37.

Wagner, H., 1932. "Transportation phenomena associated with impacts and sliding on liquid surfaces," *Journal of Mathematical Methods,* **12**(4), pp. 193-215.

Wang, J. T., and Lyle, K. H., 2007. "Simulating space capsule water landing with explicit finite element method," *48th AIAA/ASME Conference*, pp. 23-26, Waikiki, HI, USA.

Wierzbicki, T., and Yue, D. K., 1986. "Impact damage of the challenger crew compartment," *Journal of Spacecraft and rockets,* **23**, pp. 646-654.

Wriggers, P., 2002. "Computational Contact Mechanics," John Wiley & Sons Ltd.

Wriggers, P., and Nackenhorst, U., 2005. "Analysis and Simulation of Contact Problems," Springer

Zhao, R., and Faltinsen, O., 1993. "Water entry of two-dimensional bodies," Journal of Fluid Mechanics, **246**, pp. 593-612.

Appendices

Appendix–A: Inertial properties of the WLO model

The inertial properties of WLO model include the following calculations:

Centre of Gravity Calculations (V_{CG}):

Distance, Z_1 = 0.06 m

Distance, Z_2 = 0.20m

Tension in Rope 1, T_1 = 0.750 kg

Tension in Rope 1, T_2 = 1.271 kg

Mass of the Model, W = 2.030 kg

$V_{CG} = Z_1 + T_2 (Z_2 - Z_1)/W$ or

$V_{CG} = Z_2 - T_1 (Z_2 - Z_1)/W$ from top of the body

= 147.8 mm from nose of the model

Details of Moment of Inertia Calculations (I_{xx}):

Mass of the model + Pendulum,	m_1	=	12.43kg
Mass of the Pendulum	m_2	=	10.40kg
Mass of the model	m	=	2.03kg
Length of the Pendulum for m_1,	L_1	=	1.627m
Length of the Pendulum for m_2,	L_2	=	0.725m
Vertical Centre of Gravity,	V_{CG}	=	147.8mm
Dist. from Bearing to Model CG,	L	=	0.848m
Time Period for m_1,	t_1	=	2.3835sec
Time Period for m_2,	t_2	=	1.9480sec

$$I_o = \frac{t_1^2 m_1 g L_1}{4\pi^2} - \frac{t_2^2 m_2 g L_2}{4\pi^2}$$

$$I_{xx} = I_o - mL^2 = 0.02173 \text{ kg m}^2$$

Moment of Inertia Calculations (I_{yy}):

Mass of the Body + Pendulum,	m_1	=	12.43kg
Mass of the Pendulum,	m_2	=	10.40kg
Mass of the Body,	m	=	2.030kg
Length of the Pendulum for m_1,	L_1	=	1.627m
Length of the Pendulum for m_2,	L_2	=	0.725m
Vertical Centre of Gravity,	V_{CG}	=	147.8mm
Dist. From Bearing to Model CG,	L	=	0.848mm
Time Period for m_1,	t_1	=	2.398sec
Time Period for m_2,	t_2	=	1.992sec

$$I_o = \frac{t_1^2 m_1 g L_1}{4\pi^2} - \frac{t_2^2 m_2 g L_2}{4\pi^2}$$

$$I_{yy} = I_o - mL^2 = \underline{0.021892} \text{ kg m}^2$$

Moment of Inertia Calculations (I_{zz}):

Mass of the Body + Pendulum,	m_1	=	10.13kg
Mass of the Pendulum,	m_2	=	8.10kg
Mass of the Body,	m	=	2.03kg
Length of the Pendulum for m_1,	L	=	1.692m
Vertical Centre of Gravity,	V_{CG}	=	147.8mm
Distance between Suspenders,	b	=	340mm
Time Period for m_1,	t_1	=	2.180sec
Time Period for m_2,	t_2	=	2.240sec

$$I_{zz} = \frac{(T_1 b)^2 m_1 g}{4(2\pi)^2 L} = \underline{0.1852} \text{ kgm}^2$$

Mass moment inertia of attachments $I_{zz}^2 = \underline{0.17113}$ kgm^2

Yaw moment of inertia = $I_{zz}^1 - I_{zz}^2 = \underline{0.01402}$ kg m^2

Results

Centre of Gravity

Vertical centre of gravity of fabricated WLSC model (measured from nose) =147.8mm

Moments of Inertia

Moment of inertia of the model with respect to major (X) axis (I_{xx}) =0.02173 kg m^2

Moment of inertia of the model with respect to minor (Y) axis (I_{yy}) =0.02189 kg m^2

Moment of inertia of the model with respect to vertical (Z) axis (I_{zz}) =0.01402 kg m^2

Appendix-B: Truncated LS-DYNA input deck for the WLO impact problem

```
$# LS-DYNA Keyword file created by LS-PREPOST 2.4 - 20Feb2010(13:51)
$# Created on September-27-2010 (18:11:53)
*KEYWORD
*TITLE
LS-DYNA USER INPUT
*ALE_MULTI-MATERIAL_GROUP
$#     sid    idtype
       2         1
*ALE_MULTI-MATERIAL_GROUP
$#     sid    idtype
       3         1
*BOUNDARY_NON_REFLECTING
$#    ssid       ad       as
       1    0.000    0.000
*BOUNDARY_SPC_SET_ID
$#      id                                          heading
       0Fix_XYZ_Bottom
$#    nsid      cid     dofx     dofy     dofz    dofrx    dofry    dofrz
       2         0        1        1        1        1        1        1
*SET_NODE_LIST_TITLE
Fix_XYZ_Bottom
$#     sid      da1      da2      da3      da4
       2    0.000    0.000    0.000    0.000
$#    nid1     nid2     nid3     nid4     nid5     nid6     nid7     nid8
     2573     2574     2613     2653     2694     2733     2734     2754
     2793     2814     2854     2874     2913     2914     2934     2973
*BOUNDARY_SPC_SET_ID
$#      id                                          heading
       0Fix_YZ_Top
$#    nsid      cid     dofx     dofy     dofz    dofrx    dofry    dofrz
       3         0        0        1        1        0        0        0
*SET_NODE_LIST_TITLE
Fix_YZ_Top
$#     sid      da1      da2      da3      da4
       3    0.000    0.000    0.000    0.000
$#    nid1     nid2     nid3     nid4     nid5     nid6     nid7     nid8
    19933    19934    19973    20013    20054    20093    20094    20114
    20153    20174    20214    20234    20273    20274    20294    20333
*BOUNDARY_SPC_SET_ID
$#      id                                          heading
       0Fix_Z
$#    nsid      cid     dofx     dofy     dofz    dofrx    dofry    dofrz
       4         0        0        0        1        0        0        0
*SET_NODE_LIST_TITLE
Fix_Z
$#     sid      da1      da2      da3      da4
       4    0.000    0.000    0.000    0.000
```

```
$#    nid1      nid2      nid3      nid4      nid5      nid6      nid7      nid8
     1627      1628      1629      1631      1633      1636      1639      1643
     1647      1652      1657      1664      1670      1679      1686      1696
*CONSTRAINED_LAGRANGE_IN_SOLID
$#   slave    master     sstyp     mstyp     nquad     ctype     direc     mcoup
       1         1         1         0         4         4         1         1
$#   start       end      pfac      fric    frcmin      norm   normtyp      damp
    0.0001.0000E+10  0.100000     0.000  0.500000         0         0     0.000
$#      cq      hmin      hmax     ileak     pleak   lcidpor     nvent  blockage
    0.000     0.000     0.000         0  0.010000         0         0         0
$#  iboxid   ipenchk   intforc   ialesof    lagmul    pfacmm      thkf
       0         0         0         0     0.000         0     0.000
*CONTROL_ALE
$#     dct      nadv      meth      afac      bfac      cfac      dfac      efac
       3         1         1 -1.000000     0.000     0.000     0.000     0.000
$#   start       end     aafac     vfact      prit       ebc      pref   nsidebc
    0.0001.0000E+20  1.000000 1.0000E-6         0         0     0.000         0
*CONTROL_TERMINATION
$# endtim    endcyc    dtmin    endeng    endmas
  1.000000         0     0.000     0.000     0.000
*CONTROL_TIMESTEP
$# dtinit    tssfac      isdo    tslimt     dt2ms      lctm     erode     ms1st
    0.000  0.900000         0     0.000     0.000         0         0         0
$#  dt2msf   dt2mslc     imscl
    0.000         0         0
*DATABASE_MATSUM
$       DT
$#      dt    binary      lcur     ioopt
 3.0000E-4         0         0         1
*DATABASE_RCFORC
$       DT
$#      dt    binary      lcur     ioopt
 1.0000E-4         0         0         1
*DATABASE_BINARY_D3PLOT
$#      dt      lcdt      beam     npltc    psetid
  0.010000         0         0         0         0
$#   ioopt
       0
*DEFINE_CURVE_TITLE
Gravity
$#    lcid      sidr       sfa       sfo      offa      offo    dattyp
       1         0  1.000000  1.000000     0.000     0.000         0
$#              a1                o1
           0.000          9.8100004
       100.0000000          9.8100004
*ELEMENT_SOLID
$#   eid     pid      n1      n2      n3      n4      n5      n6      n7      n8
     1       2    2495    2496    2497    2498    1627    1629    1634    1630
     2       2    2499    2500    2501    2502    2495    2496    2497    2498
*EOS_GRUNEISEN_TITLE
Water
```

```
$#   eosid       c       s1       s2       s3     gamao         a        e0
       1 100.00000     0.000     0.000     0.000     0.000     0.000     0.000
$#      v0
    0.000
*INITIAL_VELOCITY_GENERATION
$#nsid/pid      styp     omega        vx        vy        vz     ivatn
       1         3     0.000     0.000     0.000 -9.810000         0
$#      xc        yc        zc        nx        ny        nz     phase    iridid
    0.000     0.000     0.000     0.000     0.000     0.000         0         0
*LOAD_BODY_Z
$#    lcid        sf    lciddr        xc        yc        zc       cid
       1  1.000000         0     0.000     0.000     0.000         0
*MAT_RIGID_TITLE
WLO
$^M-1
$      MID        RO         E        PR         N    COUPLE         M     ALIAS
$#     mid        ro         e        pr         n    couple         m     alias
       1  2.0800002.0700E+11  0.300000     0.000     0.000     0.0000.0
$#     cmo      con1      con2
    0.000         0         0
$# lco or a1       a2        a3        v1        v2        v3
    0.000     0.000     0.000     0.000     0.000     0.000
*MAT_NULL_TITLE
Water
$#     mid        ro        pc        mu     terod     cerod        ym        pr
       2 100.00000     0.000     0.000     0.000     0.000     0.000     0.000
*MAT_VACUUM_TITLE
Air
$#     mid       den
       3     0.000
*NODE
$#   nid               x             y             z      tc      rc
     1     -0.0010522     -0.1647336      0.5361838       0       0
     2     -0.0010106     -0.1608027      0.5268745       0       0
     3     -0.0188286     -0.1598454      0.5268390       0       0
     4     -0.0184644     -0.1637675      0.5361818       0       0
*PART
$# title
WLO
$#     pid     secid       mid     eosid      hgid      grav    adpopt      tmid
       1         1         1         0         0         1         1         0
*SECTION_SHELL_TITLE
WLO
$^P-1
$    SECID    ELFORM      SHRF       NIP     PROPT   QR/IRID     ICOMP     SETYP
$#   secid    elform      shrf       nip     propt   qr/irid     icomp     setyp
       1         2  1.000000         2         1         0         0         1
$#      t1        t2        t3        t4      nloc     marea      idof    edgset
  0.005000  0.005000  0.005000  0.005000     0.000     0.000     0.000         0
*PART
$# title
```

```
Water
$#     pid     secid       mid     eosid      hgid      grav    adpopt      tmid
         2         2         2         1         0         0         0         0
*SECTION_SOLID_ALE_TITLE
Water
$#   secid    elform       aet
         2        11         0
$#    afac      bfac      cfac      dfac     start       end     aafac
    0.000     0.000     0.000     0.000     0.000     0.000     0.000
*PART
$# title
Air
$#     pid     secid       mid     eosid      hgid      grav    adpopt      tmid
         3         3         3         0         0         0         0         0
*SECTION_SOLID_ALE_TITLE
Air
$#   secid    elform       aet
         3        11         0
$#    afac      bfac      cfac      dfac     start       end     aafac
    0.000     0.000     0.000     0.000     0.000     0.000     0.000
*SET_NODE_LIST_TITLE
WLO
$#     sid       da1       da2       da3       da4
         1     0.000     0.000     0.000     0.000
$#    nid1      nid2      nid3      nid4      nid5      nid6      nid7      nid8
         1         2         3         4         5         6         7         8
         9        10        11        12        13        14        15        16
        17        18        19        20        21        22        23        24
        25        26        27        28        29        30        31        32
*SET_PART_LIST_TITLE
Water and Air
$#     sid       da1       da2       da3       da4
         1     0.000     0.000     0.000     0.000
$#    pid1      pid2      pid3      pid4      pid5      pid6      pid7      pid8
         2         3         0         0         0         0         0         0
*SET_SEGMENT_TITLE
Water and Air Radial
$#     sid       da1       da2       da3       da4
         1     0.000     0.000     0.000     0.000
$#      n1        n2        n3        n4        a1        a2        a3        a4
     33025     33026     33666     33665     0.000     0.000     0.000     0.000
     27839     27841     27161     27159     0.000     0.000     0.000     0.000
     27544     26904     26906     27546     0.000     0.000     0.000     0.000
     24719     24721     24101     24099     0.000     0.000     0.000     0.000
     23344     22824     22826     23346     0.000     0.000     0.000     0.000
*END
```